Am J Physiol Endocrinol Metab 298: E1058–E1071, 2010.
First published February 16, 2010; doi:10.1152/ajpendo.00773.2009.

Contraction-related stimuli regulate GLUT4 traffic in C_2C_{12}-GLUT4*myc* skeletal muscle cells

Wenyan Niu,[1,2] Philip J. Bilan,[1] Shuhei Ishikura,[1] Jonathan D. Schertzer,[1] Ariel Contreras-Ferrat,[1,3] Zhengxiang Fu,[2] Jie Liu,[2] Shlomit Boguslavsky,[1] Kevin P. Foley,[1] Zhi Liu,[1] Jinru Li,[2] Guilan Chu,[2] Thomas Panakkezhum,[5] Gary D. Lopaschuk,[5] Sergio Lavandero,[3,4] Zhi Yao,[2] and Amira Klip[1]

[1]*Program in Cell Biology, The Hospital for Sick Children, Toronto, Ontario, Canada;* [2]*Department of Immunology, Key Laboratory of Immuno Microenvironment and Disease of the Educational Ministry of China, Tianjin Medical University, Tianjin, China;* [3]*Centro Estudios Moleculares de la Célula, Facultad Ciencias Quimicas y Farmaceuticas;* [4]*Instituto de Ciencias Biomédicas, Facultad de Medicina, Universidad de Chile, Santiago, Chile; and* [5]*Cardiovascular Research Group, Mazankowski Alberta Heart Institute, University of Alberta, Edmonton, Alberta, Canada*

Submitted 24 December 2009; accepted in final form 16 February 2010

Niu W, Bilan PJ, Ishikura S, Schertzer JD, Contreras-Ferrat A, Fu Z, Liu J, Boguslavsky S, Foley KP, Liu Z, Li J, Chu G, Panakkezhum T, Lopaschuk GD, Lavandero S, Yao Z, Klip A. Contraction-related stimuli regulate GLUT4 traffic in C_2C_{12}-GLUT4*myc* skeletal muscle cells. *Am J Physiol Endocrinol Metab* 298: E1058–E1071, 2010. First published February 16, 2010; doi:10.1152/ajpendo.00773.2009.—Muscle contraction stimulates glucose uptake acutely to increase energy supply, but suitable cellular models that faithfully reproduce this complex phenomenon are lacking. To this end, we have developed a cellular model of contracting C_2C_{12} myotubes overexpressing GLUT4 with an exofacial *myc*-epitope tag (GLUT4*myc*) and explored stimulation of GLUT4 traffic by physiologically relevant agents. Carbachol (an acetylcholine receptor agonist) induced a gain in cell surface GLUT4*myc* that was mediated by nicotinic acetylcholine receptors. Carbachol also activated AMPK, and this response was sensitive to the contractile myosin ATPase inhibitor *N*-benzyl-*p*-toluenesulfonamide. The gain in surface GLUT4*myc* elicited by carbachol or by the AMPK activator 5-amino-4-carboxamide-1 β-ribose was sensitive to chemical inhibition of AMPK activity by compound C and partially reduced by siRNA-mediated knockdown of AMPK catalytic subunits or LKB1. In addition, the carbachol-induced gain in cell surface GLUT4*myc* was partially sensitive to chelation of intracellular calcium with BAPTA-AM. However, the carbachol-induced gain in cell surface GLUT4*myc* was not sensitive to the CaMKK inhibitor STO-609 despite expression of both isoforms of this enzyme and a rise in cytosolic calcium by carbachol. Therefore, separate AMPK- and calcium-dependent signals contribute to mobilizing GLUT4 in response to carbachol, providing an in vitro cell model that recapitulates the two major signals whereby acute contraction regulates glucose uptake in skeletal muscle. This system will be ideal to further analyze the underlying molecular events of contraction-regulated GLUT4 traffic.

carbachol; glucose transporter 4; adenosine 5′-monophosphate-activated protein kinase; acetylcholine

SKELETAL MUSCLE IS A MAJOR DETERMINANT OF GLYCEMIA, and insulin and exercise are two major physiological stimuli of glucose uptake into this tissue. For both insulin and acute muscle contraction, this occurs through redistribution of GLUT4 from vesicle storage compartments to the plasma membrane (7, 14). Signals emanating from the insulin receptor leading to glucose uptake include insulin receptor substrate-1, phosphatidylinositol 3-kinase, Akt, and the Rab-GAP protein AS160 (9, 26, 34, 40, 78). In contrast, the signaling pathways by which muscle contraction regulates GLUT4 vesicle traffic remain poorly defined, since studies have so far been confined to analyzing pathways involved in the stimulation of glucose uptake in intact muscle tissue (4, 16, 30, 54, 55). Those studies reveal participation of signals requiring calcium and AMP-dependent protein kinase (AMPK) in the stimulation of glucose transport (20, 28, 48, 76, 77). Cytosolic calcium rises rapidly in response to the depolarizing excitatory signal and consequent calcium release from the sarcoplasmic reticulum. Such calcium triggers myosin II-dependent mechanical contraction and relaxation cycles that consume ATP, in turn activating AMPK (1). Accordingly, pre- and postforce production signals appear to contribute to the stimulation of glucose uptake. Calcium may signal through a variety of calcium-sensitive kinases, such as calmodulin-dependent kinase II (CaMKII) or protein kinase C, or it may contribute to activation of AMPK through its upstream activator CaMK kinase (CaMKK) (25, 28). Alternatively, AMPK is also activated directly by its classical upstream activator LKB1 in response to a rise in AMP (18, 75). Thus, AMPK appears to play a central role, and numerous studies provide evidence for and against participation of each of these kinases in the stimulation of glucose uptake by contraction (10, 28, 29, 31, 41, 45, 76, 77), depending partly on the contraction protocol, muscle type, and method of analysis.

We hypothesize that there is a need to establish a simplified cellular model amenable to physiological stimulation and contraction in which to obtain proof of principle for the participation of individual pathways, their effect on GLUT4 traffic in addition to glucose uptake, and their possible interplay. Although L6 muscle cells have proven extremely useful to dissect out insulin signals and their impact on GLUT4 traffic, C_2C_{12} myotubes may be more suitable to study contraction signal transduction as only they develop a contractile apparatus of sarcomere units (11, 43, 49). In addition, C_2C_{12} myotubes have abundant levels of nicotinic acetylcholine receptors that are organized into signaling clusters upon ligand binding (21, 71). Yet, C_2C_{12} myotubes have not been widely utilized to study insulin- or contraction-stimulated glucose uptake because they express extremely low levels of GLUT4 (37). A line of C_2C_{12} cells transfected with GLUT4 was recently used to study the effect of chronic electrical pulse stimulation on cytokine production and GLUT4 cycling (49) but not explored for their acute response to muscle contraction. Here, we stably overexpress GLUT4 with a *myc* epitope in its first exofacial loop

Address for reprint requests and other correspondence: P. J. Bilan, Program in Cell Biology, The Hospital for Sick Children, McMaster Bldg., Rm. 5006E, 555 University Ave., Toronto, ON, M5G 1X8, Canada (e-mail: pbilan@sickkids.ca).

(GLUT4*myc*) into the C_2C_{12} myoblast background and characterize the ability of cholinergic stimulation via carbachol to increase GLUT4*myc* at the surface of differentiated myotubes. Using this system, we demonstrate that carbachol increases cytosolic calcium and activates AMPK in a myosin II-ATPase-dependent manner. The cholinergic agonist induces an increase in GLUT4*myc* at the cell surface that depends in part on AMPK and in part on a calcium-induced signal that may involve CaMKII. Thus, this cellular system responds to a physiological trigger of muscle contraction by activating calcium and AMPK signals that converge on rapidly increasing surface GLUT4 levels.

MATERIALS AND METHODS

Materials. Human insulin (Humulin R) was obtained from Eli Lilly Canada (Toronto, ON, Canada). 2-Deoxy-D-[^{3}H]glucose (25–50 Ci/mmol, NET-549) and D-[^{14}C]mannitol (56 Ci/mmol, NEC-314) were purchased from PerkinElmer (Waltham, MA). Indinavir was obtained from Merck Research Laboratories (Rahway, NJ) through a materials transfer agreement. Cytochalasin B, β-D-glucose, 2-deoxy-D-glucose, *o*-phenylenediamine dihydrochloride, carbamoylcholine chloride (carbachol), protease inhibitor cocktail, polyclonal IgG to c-*myc* (epitope), IgM to α-actinin-1, α-bungarotoxin, epibatidine, atropine, and all purest grade available chemicals were from Sigma Chemical (St. Louis, MO) unless otherwise noted. Fluo 3-AM, pluronic F-127, lipofectamine 2000 and lipofectamine RNAiMax, GIBCO brand horse serum, Alexa 488-conjugated goat anti-mouse IgG, Zymed brand transferrin receptor antibody, and TRIzol were from Invitrogen (Carlsbad, CA). All small interfering RNA (siRNA) oligonucleotides were from Qiagen. Compound C, KN93, 1,2-bis-(*o*-aminophenoxy)ethane-*N,N,N′,N′*-tetraacetic acid tetraacetoxymethyl ester (BAPTA-AM), and blasticidin-S-hydrochloride were from Calbiochem (San Diego, CA). AICAR was from BioMol (Plymouth Meeting, PA). *N*-benzyl-*p*-toluenesulfonamide (BTS) was from Toronto Research Chemicals (Toronto, On, Canada). STO-609 was from Tocris Bioscience (Ellisville, MO). Pierce BCA protein detection kit was from Thermo Fisher Scientific (Rockford, IL). Dulbecco's modified Eagle's medium (DMEM), α-MEM, fetal bovine serum (FBS), penicillin-streptomycin, and trypsin-EDTA were from Wisent (St.-Bruno, QC, Canada). Monoclonal anti-*myc* (9E10) was from Santa Cruz Biotechnology (Santa Cruz, CA). Anti-AMPKα1, anti-AMPKα2, and anti-insulin-responsive aminopeptidase (IRAP) antibodies were from Millipore (Lake Placid, NY). Anti-pan-AMPKα, anti-AMPK (Thr^{172}), and anti-phospho-acetyl-CoA carboxylase (ACC; Ser^{79}) were from Cell Signaling Technology (Danvers, MA). Anti-sortilin was from BD Biosciences. Anti-vesicle-associated membrane protein (VAMP)2 was from Affinity BioReagents. Anti-VAMP7 was kindly provided by Thierry Galli (INSERM, Paris, France). Antibodies to glucose transporter (GLUT)1 and GLUT4 were prepared by immunization of rabbits with keyhole limpet hemocyanin conjugated to peptides representing the last 12 amino acids of rat GLUT1 or GLUT4 (61). Horseradish peroxidase (HRP)-bound goat anti-mouse, goat anti-rabbit IgG, and donkey anti-mouse IgM antibodies were from Jackson ImmunoResearch Laboratories (West Grove, PA). Western Lightning Chemiluminescence Reagent Plus was from PerkinElmer, (Boston, MA), and HyBlot CL autoradiography film was from Denville Scientific (Metuchen, NJ).

C_2C_{12}-GLUT4myc cell line. Briefly, GLUT4*myc* cDNA (from *Rattus norvegicus*) was constructed by inserting the human c-*myc* epitope (14 codons for AEEQKLISEEDLLK) between codons 66 and 67 (the 1st ectodomain of GLUT4) and subcloned into the pCXN2 vector (32). C_2C_{12} myoblasts were transfected using 2 μg of DNA/well of a six-well plate, using Lipofectamine 2000 according to the product manual. Stably transfected clones were selected in growth medium containing blasticidin at 10 μg/ml after each six-well plate was split into a 10-cm-diameter dish. Colonies were selected with cloning cylinders, and ~50 clones were screened for high GLUT4*myc* protein expression and superior fusion into myotubes. One clone of C_2C_{12}-GLUT4*myc* myoblasts was selected for further characterization in this study.

Cell culture. C_2C_{12}-GLUT4*myc* myoblasts were maintained in DMEM containing 4.5 g/l glucose supplemented with 10% FBS (vol/vol), 30 μg/ml penicillin, 100 μg/ml streptomycin, and 5 μg/ml blasticidin in a humidified atmosphere of air and 5% CO_2 at 37°C. Myoblasts seeded at 4×10^4 cells/well were allowed to reach confluence and then differentiated into myotubes in DMEM (4.5 g/l glucose) supplemented with 5% horse serum (vol/vol), penicillin, and streptomycin. Myotubes were used within 7–8 days after seeding. Wild-type C_2C_{12} cells were cultured in medium without blasticidin. L6-GLUT4*myc* myoblasts were maintained in α-MEM with 10% FBS (vol/vol), 1% antibiotics-antimycotic (vol/vol), and 2.5 μg/ml blasticidin in an atmosphere supplemented with 5% CO_2 at 37°C. For differentiation into myotubes, L6-GLUT4*myc* myoblasts were seeded in α-MEM containing 2% FBS (vol/vol) and 1% antibiotics/antimycotic (vol/vol) at 2×10^4 cells/ml. Full L6 differentiation occurred 6–8 days after seeding. Wild-type L6 cells were cultured without blasticidin. For experiments involving microscopy (e.g., Ca^{2+} measurements, immunofluorescence), C_2C_{12}-GLUT4*myc* or L6-GLUT4*myc* myoblasts or myotubes were grown on glass coverslips. In addition, cultures were grown in six-well plates for protein extraction or 24-well plates for all other assays. Cells were depleted of serum for 4.5 h prior to all assays. Pretreatments with inhibitors and treatments with stimuli were timed so their completion would coincide with the end of the serum depletion period of 4.5 h. Inhibitors were administered in DMSO as vehicle so that the final concentration did not exceed 0.01% (vol/vol). DMSO was without effect on any of the parameters assayed.

Cell lysates and immunoblotting. Briefly, C_2C_{12}-GLUT4*myc* or L6-GLUT4*myc* myotubes grown in six-well plates were incubated as indicated and lysed on ice with 300 μl of RIPA buffer (100 mM NaCl, 0.25% wt/vol sodium deoxycholate, 1.0% wt/vol NP-40, 0.1% wt/vol SDS, 2 mM EDTA, 50 mM NaF, 10 nM okadaic acid, 1 mM sodium orthovanadate, protease inhibitor cocktail, and 50 mM Tris·HCl, pH 7.2). Aliquots of the lysates were mixed with 5× Laemmli sample buffer supplemented with β-mercaptoethanol at a final concentration of 7.5% (vol/vol). The lysates were then heated for 15 min at 65°C. Equal amounts of protein samples were resolved by 7.5% SDS-PAGE, transferred to polyvinylidene difluoride membranes (Bio-Rad, Hercules, CA), and immunoblotted with the following primary antibodies: GLUT1 (1:1,000), GLUT4 (1:1,000), c-*myc* (9E10, 1:250), transferrin receptor (1:1,000), IRAP (1:1,000), sortilin (1:2,000), VAMP2 (1:1,000), VAMP7 (1:1,000), AMPKα1 (1:1,000), AMPKα2 (1:1,000), pan-AMPKα (1:1,000), phospho-Thr^{172} AMPKα (1:1,000), ACC (1:1,000), phospho-Ser^{79} ACC (1:1,000), LKB1 (1:1,000), and α-actinin 1 (1:20,000). Primary antibodies were detected with appropriate HRP-conjugated antibodies, and the chemiluminescent signal was developed with autoradiographic film. Densitometric quantification of protein bands was performed using National Institutes of Health (NIH) Image J software.

Cell membrane preparation. C_2C_{12}-GLUT4*myc* myotubes grown in two 25-cm^2-dishes were scraped in ice-cold PBS and transferred into a 50-ml Falcon tube for centrifugation (700 *g*, 5 min, 4°C) to pellet intact cells. Pellets were resuspended in 4 ml of homogenization buffer containing 255 mM sucrose, 2 mM Na_2 EDTA, and 20 mM HEPES (pH 7.4) supplemented with protease inhibitor cocktail and homogenized with 15 strokes in a 10-ml glass A-type Dounce homogenizer on ice. Homogenates were centrifuged (700 *g*, 10 min, 4°C) to sediment nuclei and unbroken cells, and supernatants were centrifuged at 195,000 *g* for 75 min at 4°C. This final pellet containing the total cellular membrane fraction was resuspended in 100 μl of homogenization buffer supplemented with protease inhibitor cocktail, and protein content was determined using the Pierce BCA method.

Indirect immunofluorescence. Cells grown on coverslips were rinsed twice with ice-cold PBS prior to fixation with 4% formaldehyde in PBS for 30 min, initiated at 4°C, and then shifted to room

temperature, followed by quenching with 0.1 M glycine in PBS for 10 min. Cells were permeabilized with 0.1% Triton X-100 for 20 min at room temperature before immunolabeling with anti-c-*myc* 9E10 antibody (1:200), followed by Alexa 488-conjugated goat anti-mouse IgG (Invitrogen, Carlsbad, CA) secondary antibody (1:1,000) in PBS containing 1% BSA. The cells were rinsed six times with PBS and then water. Coverslips were mounted on slides with Dako (Carpinteria, CA) solution and analyzed on a Zeiss LSM-510 laser scanning confocal microscope.

2-Deoxy-D-glucose uptake in cultured cells. Following serum depletion, cells were treated with insulin, AICAR, or carbachol in triplicate at the concentrations and times indicated. Cells were rinsed with HEPES-buffered saline (140 mM NaCl, 5 mM KCl, 2.5 mM $MgSO_4$, 1.0 mM $CaCl_2$, and 20 mM HEPES-Na, pH 7.4, 295 ± 5 mOsm) and used immediately for measurement of 2-deoxy-D-glucose uptake as described (50). Inclusion of cytochalasin B (10 μM) in some wells of the uptake assay would block transporter-mediated association of radiolabeled 2-deoxy-D-glucose with the cells. The remainder was subtracted from the total uptake to calculate glucose transporter-mediated glucose uptake. Inclusion of indinavir (100 μM) in some wells of the uptake assay was used to determine the contribution of GLUT4-mediated glucose uptake.

Cell surface GLUT4myc density. GLUT4*myc* levels at the cell surface of intact C_2C_{12}-GLUT4*myc* myotubes were measured by an antibody-coupled colorimetric assay, as described for L6-GLUT4*myc* cells (50), with modifications for C_2C_{12}-GLUT4*myc* myotubes. Briefly, cells grown in 24-well plates and serum depleted for 4.5 h and treated as indicated were washed twice with ice-cold PBS and fixed with 3% (vol/vol) paraformaldehyde for 10 min at 4°C and 20 min at room temperature. All subsequent steps were at room temperature. Cells were rinsed and incubated for 10 min with 0.1 M glycine in PBS. Following blocking with 5% nonfat milk (wt/vol) in PBS for 10 min, cells were reacted with anti-*myc* polyclonal antibody (1:250) in 5% milk in PBS for 1 h. After five washes with PBS, cells were incubated with HRP-conjugated goat anti-rabbit IgG (1:5,000) for 1 h, washed extensively with PBS (6 times, 1 ml/well, 3 min/wash), and incubated with 1 ml/well of 0.4 mg/ml *o*-phenylenediamine dihydrochloride reagent for 20 min. The reaction was stopped by addition of 0.25 ml of 3 N HCl. Supernatant was collected and 0.2 ml used to read optical absorbance at 492 nm. Background absorbance obtained from wild-type C_2C_{12} myotubes was subtracted from all values.

Mouse skeletal muscle 2-deoxy-D-glucose uptake and homogenates. Extensor digitorum longus (EDL) hindlimb skeletal muscles were removed by dissection (62) from mice anesthetized with 100 μl/10 g body wt of 100 mg·ml ketamine^{-1}·25 mg^{-1}·ml^{-1} xylazine mixture by intraperitoneal injection, in accordance with a protocol approved by the Animal Care Committee at The Hospital for Sick Children. Prior to 2-deoxy-D-glucose uptake (15), muscles were equilibrated in gassed (95% O_2, 5% CO_2) Krebs-Ringer bicarbonate (KRB) buffer (137 mM NaCl, 5 mM KCl, 1 mM $MgSO_4$, 1 mM $CaCl_2$, 1 mM $NaH2PO_4$, 24 mM $NaHCO_3$) containing 32 mM D-mannitol, 8 mM D-glucose, and 0.1% fatty acid-free BSA for 30 min in a rotating water bath (110 rpm, 30°C), followed by incubation with carbachol, insulin, or AICAR (at 100 μM, 10 nM, or 2 mM, respectively, for 30 min). Muscles were rinsed for 10 min in the presence of inhibitors and stimulators in KRB buffer without glucose containing 40 mM D-mannitol and 0.1% fatty acid-free BSA. 2-Deoxy-D-[^{3}H]glucose uptake (2.25 μCi/ml) was performed for 20 min at 29°C in KRB buffer containing 7.3 mM 2-deoxy-D-glucose supplemented with 32 mM D-mannitol (plus 0.3 μCi/ml D-[^{14}C]mannitol), 2 mM pyruvic acid, and 0.1% BSA. Muscles were blotted on filter paper, weighed, and lysed in 1 ml of 1 M NaOH for 1 h at 85°C, followed by liquid scintillation counting. Extracellular trapping and glucose transporter-independent uptake were calculated using the nontransportable D-[^{14}C]mannitol. Muscle homogenates were prepared following incubation with stimulators by homogenization in 0.3 ml of 255 mM sucrose, 2 mM Na_2EDTA, 20 mM HEPES (pH 7.4) supplemented with protease inhibitor cocktail, 1 mM sodium vanadate, 10 nM okadaic acid, and 50 mM NaF using 20 strokes with a 5-ml Wheaton glass homogenizer. Homogenates were transferred to microtubes and centrifuged at 8,000 *g* for 10 min at 4°C, and the pellet was discarded. Protein concentrations were determined using the BCA method.

siRNA. C_2C_{12}-GLUT4*myc* myotubes were transfected with siRNA to nonrelated control or LKB1 or cotransfected with siRNA to AMPKα1 and -α2 (total 200 nM oligonucleotide) using the lipofectamine RNAiMax transfection reagent per the manufacturer's instructions. The target sequences for siRNA oligomers for AMPKα1, AMPKα2, and LKB1 were AAG GAA AGT GAA GGT GGG CAA (gene ID: 105787), TTC CCT TTC ATT AAT CCT TTA (gene ID: 108079), and CAG CTG ATT GAC GGC CTG GAA (gene ID: 20869), respectively. The sense sequence for nonrelated siRNA control was AUU CUA UCA CUA GCG UGA C dTdT. Cells were transfected on *days 4* and *5* after seeding, and experiments were carried out 72 h posttransfection.

Determination of intracellular Ca^{2+}. C_2C_{12}-GLUT4*myc* myotubes grown on coverslips were serum deprived in DMEM for 3 h and then washed three times with Ca^{2+}-containing resting buffer (145 mM NaCl, 5 mM KCl, 2.6 mM $CaCl_2$, 1 mM $MgCl_2$, 5.6 mM D-glucose, and 10 mM HEPES, pH 7.4) and loaded with 10 μM Fluo 3-AM calcium-sensitive fluorescent dye (stock in 20% pluronic acid, DMSO) for 50 min at 37°C. After dye loading, cells were washed with resting buffer and used within 1 h. Coverslips were mounted in a 1-ml-capacity temperature-controlled chamber (37°C) and placed in the microscope for fluorescence measurements (excitation 490 nm). Recording of fluorescent images was initiated ≥5 min prior to direct addition of carbachol to the chamber at the final concentrations indicated, and images were collected every 1.3 s with a PL APO 40×/1.25–0.75 objective using Meta Imaging Series 6.1 software by Molecular Devices (Sunnyvale, CA). For quantification of the fluorescence in each cell, a manual contour was generated and the mean of fluorescence intensity calculated. Intracellular concentrations of Ca^{2+} were expressed as percentages of fluorescence intensity relative to basal (a value stable for ≥5 min in resting conditions). The fluorescence intensity increase is proportional to the rise in intracellular calcium.

Microscopy, time-lapse movies, and image analysis. Cells were plated on 25-mm cover glasses (VMR, Natick, MA). A Leica DM IRE2 microscope (with a PL-APO 40×/1.25 oil objective) and a temperature controller (Medical Systems, Greenvale, NY) were used along with a Hamamatsu (Shizuoka, Japan) model C4742-95-12ER charge-coupled device camera. Volocity 5.0 software was used to capture live-cell differential interference contrast images at 10 frames/s for a period of 20 and 11 min for carbachol/vehicle- and carbacol/BTS-treated cells, respectively. The resulting images were reassembled into one time point per 5-s movie using Volocity 5.0 software and further processed using NIH Image J 1.42 software.

mRNA extraction and RT-PCR. RNA was extracted from C_2C_{12}-GLUT4*myc* myotubes by guanidine isothiocyanate-phenol-chloroform. Semiquantitative RT-PCR was performed on 200 ng of total RNA using a Qiagen One-Step RT-PCR kit as follows: reverse transcription (50°C, 30 min), heat inactivation (95°C, 15 min), repeated cycles of denaturation (94°C, 30 s), annealing (56°C, 30 s), and extension (72°C, 60 s) with the primer pairs CaMKKα (forward, TGGAGCGTGTGTATCAGGAG; reverse, CAGGAGGTCGAACACCAAAT) and CaMKKβ (forward, TCACTCGGATGTTGGAC AAA; reverse, TCGACCAGTGTGCAGTTCTC). PCR products were subjected to 2.5% agarose gel electrophoresis in TAE buffer, ethidium bromide stained, and photographed under ultraviolet light. The number of PCR cycles was titrated for each gene-specific primer pair target to ensure linearity.

Statistical analysis. Statistical analyses were carried out using Prism 3.0 software (San Diego, CA). Two groups were compared using Student's paired *t*-test, and more than two groups were compared using analysis of variance with Tukey's post hoc analysis.

RESULTS

Characterization of the C_2C_{12}-GLUT4myc cell line. Insulin-stimulated glucose uptake and GLUT4 traffic in muscle cells have been characterized extensively, using an L6 rat muscle cell line stably transfected with a GLUT4 construct containing an exofacial *myc* epitope tag (35, 56, 70). On the other hand, L6 cells are less amenable to the study of stimuli related to muscle contraction, since they do not develop sarcomeric organization of α-actin and muscle myosin II, express low numbers of nicotinic acetylcholine receptors (51), and respond weakly to AICAR (67). These properties are better displayed by the C_2C_{12} muscle cell line, and accordingly, we generated a clonal line stably expressing GLUT4*myc* that far exceeded the low levels of endogenous GLUT4 (Fig. 1*A*). Total GLUT4 (predominantly GLUT4*myc*) expression was comparable in C_2C_{12}-GLUT4*myc* and L6-GLUT4*myc* myotubes (Fig. 1*B*). The transferrin receptor IRAP and sortilin are major membrane protein residents of the GLUT4 storage compartment (33, 42). Figure 1*C* shows that IRAP expression is higher in C_2C_{12} than in L6 myotubes, whereas the opposite was found for sortilin, a protein hypothesized to aid in sorting GLUT4 toward the insulin-sensitive storage compartment (63). VAMP2, a v-SNARE involved in regulated GLUT4 traffic (52), and VAMP7, a v-SNARE involved in the constitutive traffic of GLUT4 in unstimulated conditions (53), were similarly expressed in both cell types. Quantification of the gels in Fig. 1*C* demonstrated that the housekeeping GLUT1 glucose transporter was 1.8 ± 0.2-fold ($n = 3$) more abundant in C_2C_{12}- than L6-GLUT4*myc* myotubes. In addition, when these samples were probed with anti-myc (not shown), GLUT4*myc* content was lower in C_2C_{12} (0.5 ± 0.1; $n = 3$) compared with L6-GLUT4*myc* myotubes, suggesting that GLUT1 may contribute to some of the glucose uptake response to several stimuli in C_2C_{12}-GLUT4*myc* myotubes.

We have reported that indinavir can be used to assess the relative contributions of glucose uptake through GLUT4 (57). Indinavir is an HIV protease inhibitor that binds and inhibits GLUT4 with 100-fold higher affinity compared with other glucose transporters like GLUT1 (46). When included in the glucose uptake assay buffer, 100 μM indinavir rapidly inhibits transport through GLUT4, and cells or tissues largely dependent on GLUT4 typically show 80–90% inhibition of their glucose uptake in the presence of indinavir (57). Table 1 shows that only 17 and 41–42% of basal and stimulated rates of glucose uptake, respectively, in parental C_2C_{12} myotubes were inhibited by indinavir, suggesting significant contributions of GLUT1 to glucose uptake. In C_2C_{12}-GLUT4*myc* myotubes, indinavir inhibited 39 and 61–66% of basal and stimulated rates of glucose uptake, respectively (Table 1). These results indicate that in C_2C_{12}-GLUT4*myc* myotubes the contribution of GLUT4 to glucose uptake response was substantial. Nonetheless, GLUT1 contributed perhaps to 50% of the glucose uptake in the basal state and 25% in the stimulated states.

Previously, we estimated that the total GLUT4*myc*/GLUT1 content in L6-GLUT4*myc* cells was 500:1 based on quantification of the molar cell surface levels of GLUT1 and GLUT4, using bis-mannose affinity photolabeling and determination of the relative subcellular distributions of glucose transporters (24). By the comparisons between C_2C_{12}-GLUT4*myc* and L6-GLUT4*myc* made in Fig. 1*C* (and described above), the total GLUT4*myc*/GLUT1 content in C_2C_{12}-GLUT4*myc* myotubes is ~125:1. Assuming a large distribution of GLUT4 to intracellular membranes (24), this may suggest that a cell surface of GLUT4*myc*/GLUT1 ratio may be around 25:1.

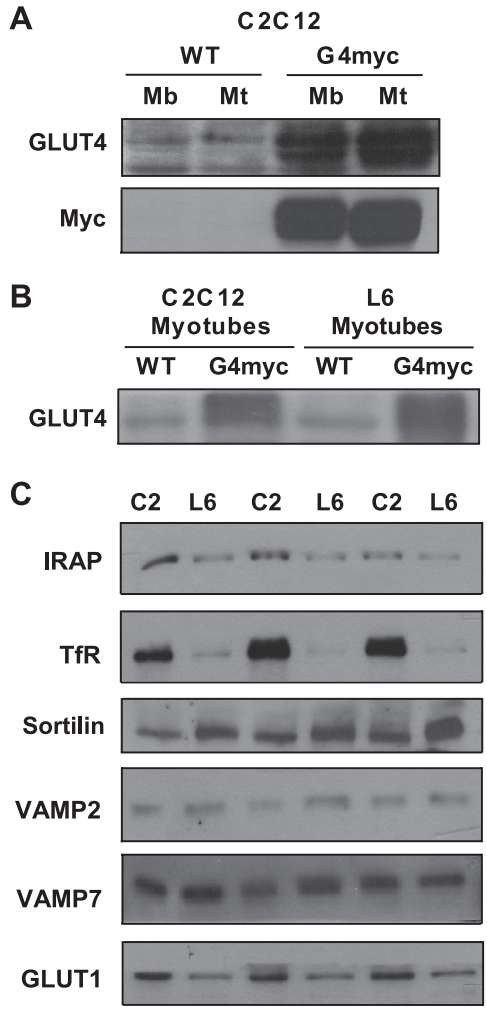

Fig. 1. Expression of GLUT4*myc* and relevant intracellular membrane proteins in C_2C_{12}-GLUT4*myc* L6-GLUT4*myc* myotubes. Cellular membranes were prepared from wild-type and GLUT4*myc*-expressing myoblasts or myotubes of C_2C_{12} or L6 cultures by homogenization, as detailed in MATERIALS AND METHODS. *A:* equal amounts of membrane protein (20 μg) from wild-type or GLUT4*myc* C_2C_{12} myoblasts (Mb) or myotubes (Mt) were immunoblotted with the c-*myc* 9E10 monoclonal antibody or GLUT4 antiserum (representative of more than 3 experiments). *B:* equal amounts of protein (20 μg) from wild-type or GLUT4*myc* C_2C_{12} or L6 myotubes were immunoblotted with GLUT4 antiserum (representative of more than 3 experiments). *C:* whole cell lysates were prepared from C_2C_{12}-GLUT4*myc* or L6-GLUT4*myc* myotubes. Equal amounts of protein (50 μg) from 3 independent C_2C_{12} (C2) or L6 culture lysates were immunoblotted for insulin-responsive aminopeptidase (IRAP), transferrin receptor (TfR), sortilin, vesicle-associated membrane protein (VAMP)2, VAMP7, and GLUT1, as designated.

Figure 2 illustrates the distribution of GLUT4*myc* in C_2C_{12} myoblasts and myotubes detected by indirect immunofluorescence via the *myc* epitope. The images show that GLUT4*myc* subcellular distribution is largely intracellular, perinuclear, and throughout the cytosol at both stages of development, similar to GLUT4*myc* distribution in L6-GLUT4*myc* cells (8).

Carbachol elevates cell surface levels of GLUT4. Motor neurons depolarize muscle fibers through the release of the neurotransmitter acetylcholine as the initiating signal for muscle contraction. Carbachol is a stable analog of acetylcholine

Table 1. *2-Deoxy-D-glucose uptake in parental and C_2C_{12}-GLUT4myc myotubes*

Treatment	Fold Above Basal		
	Glucose Uptake	Glucose Uptake Remaining After Indinavir Treatment	Inhibition by Indinavir, %
C_2C_{12}-WT			
Basal	1.00	0.83 ± 0.05	17
Insulin	1.27 ± 0.03	0.74 ± 0.06	42
AICAR	1.31 ± 0.07	0.76 ± 0.03	42
Carbachol	1.25 ± 0.08	0.74 ± 0.01	41
C_2C_{12}-GLUT4*myc*			
Basal	1.00	0.61 ± 0.04	39
Insulin	1.48 ± 0.08	0.57 ± 0.02	61
AICAR	1.63 ± 0.11	0.64 ± 0.04	61
Carbachol	1.60 ± 0.08	0.54 ± 0.09	66

Values are means ± SE. WT, wild type. Inhibition by indinavir. Myotube cultures were placed in serum-free culture medium for 4.5 h, including times of treatment (basal, no additions; insulin, 100 nM, 20 min; AICAR, 2 mM, 60 min; carbachol, 100 μM, 20 min). Cells were rinsed with HEPES-buffered saline prior to measurement of 2-deoxy-D-glucose uptake in the presence of 100 μM indinavir, 10 μM cytochalasin B, or no additions. Shown is the fold stimulation of glucose uptake relative to the respective basal rates in each cell line. Basal rate of uptake in the parental (WT) cells was 21.52 ± 2.57 pmol·mg^{-1}·min^{-1} and in the GLUT4*myc* cells was 27.64 ± 4.53 pmol·mg^{-1}·min^{-1}. Indinavir preferentially inhibits glucose from entering cells through GLUT4. The greater the %inhibition of glucose uptake by indinavir indicates greater involvement of GLUT4 in the process.

and can readily induce skeletal muscle contraction (66). When added to C_2C_{12}-GLUT4*myc* myotubes for 20 min, carbachol (0.1 mM) stimulated 2-deoxy-D-[^{3}H]glucose uptake and elevated GLUT4*myc* cell surface levels comparable with those achieved by AICAR (2 mM, 60 min) or insulin (100 nM, 20 min) (Fig. 3, *A* and *B*). Carbachol doses of 0.1–1 mM were maximally effective in raising cell surface GLUT4*myc* (not shown). Carbachol also acutely stimulated 2-deoxy-D-[^{3}H]glucose uptake in isolated mouse EDL muscles, validating it as a physiologically relevant stimulator of muscle glucose uptake (Fig. 3*C*). Like acetylcholine, carbachol activates nicotinic and muscarinic acetylcholine receptors. Although C_2C_{12} myotubes express nicotinic acetylcholine receptors (71), they also express muscle-specific muscarinic isoforms (3). To identify the acetylcholine receptor isoform involved in the carbachol response of GLUT4*myc,* agonists and antagonists of the receptors were tested. Figure 3*D* shows that the nicotinic receptor antagonist α-bungarotoxin markedly reduced the gain in cell surface GLUT4*myc* stimulated by carbachol. By contrast, the muscarinic acetylcholine receptor antagonist atropine barely affected basal and carbachol-stimulated levels of GLUT4*myc* (Fig. 3*D*). In addition, epibatidine, a potent nicotinic acetylcholine receptor agonist, significantly elevated GLUT4*myc* cell surface levels. Thus, these findings suggest that the GLUT4*myc* response to carbachol is vastly mediated by nicotinic acetylcholine receptors.

Carbachol activates AMPK in C_2C_{12} myotubes. A large body of work supports the ability of AMPK signaling to elevate glucose uptake in skeletal muscle (20, 31, 44, 45, 77). Furthermore, there is much support for a partial contribution of AMPK activity in the signaling relay of contraction-stimulated glucose uptake in this tissue (29, 41, 45, 76, 77). This may be mediated by AMPK complexes containing the α2-isoform of the enzyme, and indeed the small molecular activator of AMPK, AICAR, stimulates muscle glucose uptake, a response that is lost in AMPKα2-null mice and mice expressing a dominant inhibitory AMPK transgene in skeletal muscle (29, 31, 41, 45). C_2C_{12} myotubes express both α1- and α2-isoforms of AMPK (Fig. 4*A*). By contrast, the α2-subunit was barely detectable by immunoblotting in L6-GLUT4*myc* myotubes (Fig. 4*A*). Because the total α-subunit content detected by a pan-AMPKα antibody (that recognizes both catalytic subunit isoforms) was greater in C_2C_{12}-GLUT4*myc* than L6-GLUT4*myc* cells but the AMPKα1 subunit content was similar in both cells, these results suggest that C_2C_{12}-GLUT4*myc* myotubes express significant amounts of the AMPKα2 subunit. AICAR caused the expected phosphorylation of AMPK on the Thr^{172} regulatory site by allowing LKB1-mediated phosphorylation (59) and increased AMPK-mediated phosphorylation of its substrate ACC (Fig. 4*B*). Importantly, phosphorylation of Thr^{172} on AMPK and Ser^{79} on ACC was also elicited by carbachol, producing a stimulation of at least twofold for AMPK and threefold for ACC (Fig. 4*B*), suggesting that carbachol-activated acetylcholine receptors lead to AMPK activation. Force generation following a depolarization event induced by motor neurons or uptake of intracellular calcium from the cytosol back into the sarcoplasmic reticulum are two major ATP-consuming processes that raise AMP levels in working muscle. The myosin II ATPase inhibitor BTS reduces force generation in contracting muscle and consequently lowers AMPK activation and contraction-stimulated glucose uptake (1). Indeed, the continued presence of carbachol in C_2C_{12} myotube cultures

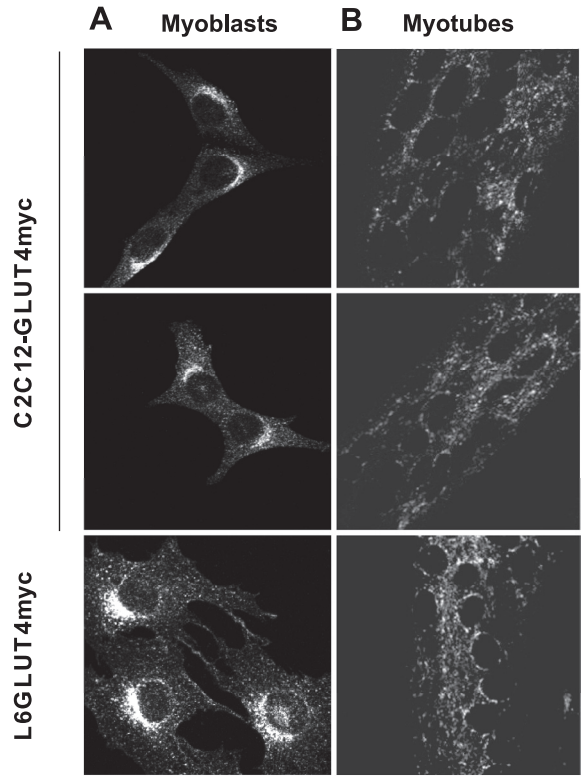

Fig. 2. Indirect immunofluorescence detection of GLUT4*myc* in C_2C_{12} myoblasts and myotubes. C_2C_{12}-GLUT4*myc* and L6-GLUT4*myc* myoblasts and myotubes were cultured on glass coverslips and fixed with paraformaldehyde in preparation for immunofluorescence detection of GLUT4*myc* using the c-*myc* 9E10 monoclonal antibody, as indicated in MATERIALS AND METHODS. Illustrated is GLUT4*myc* staining in C_2C_{12}-GLUT4*myc* and L6-GLUT4*myc* myoblasts (*A*) and myotubes (*B*). Images are representative of 3 independent experiments.

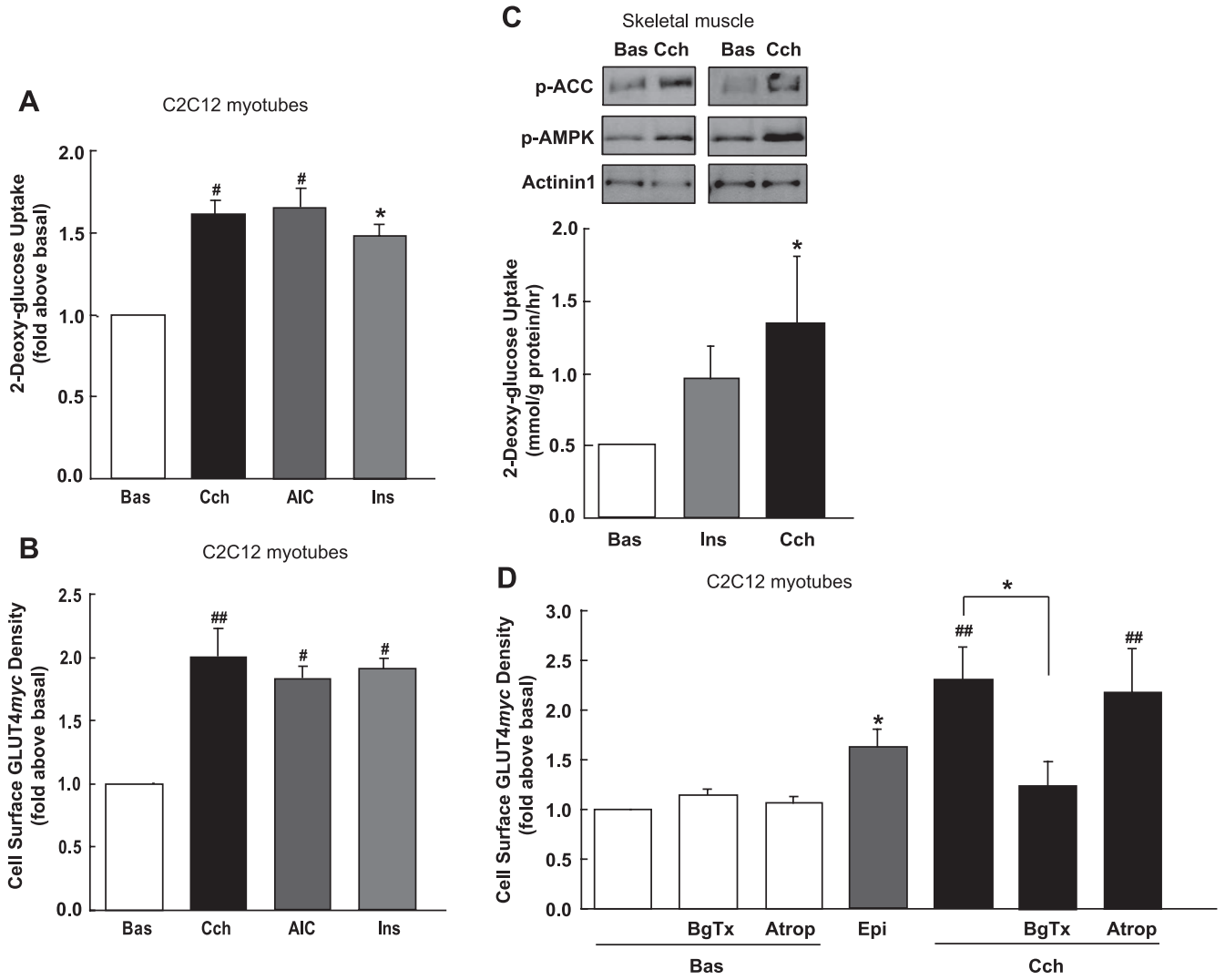

Fig. 3. Carbachol (Cch) and AICAR (AIC) stimulate glucose uptake and induce a gain of GLUT4*myc* at the surface of C_2C_{12}-GLUT4*myc* myotubes, and Cch stimulates glucose uptake into mouse extensor digitorum longus (EDL) muscle. C_2C_{12}-GLUT4*myc* myotubes were serum deprived for 4.5 h, including incubation periods with Cch (100 μM, 20 min), AIC (2 mM, 60 min), or insulin (Ins; 10 nM, 20 min) prior to measurement of 2-deoxy-D-[^{3}H]glucose uptake (*A*) or cell surface GLUT4*myc* density (*B*), as indicated in MATERIALS AND METHODS. Illustrated are the means ± SE of at least 4 independent experiments; $*P < 0.05$, $\#P < 0.01$, and $\#\#P < 0.001$ relative to basal (Bas). *C*: Cch activates AMP-activated protein kinase (AMPK) and stimulates glucose uptake in isolated mouse EDL muscle. Both hindlimb EDL muscles were surgically excised from anesthetized C57BL/6J mice and either treated with Cch (100 μM, 30 min) or had no further additions (basal) prior to immunoblotting for phospho (p)-Thr^{172} AMPK, p-Ser^{79} acetyl-CoA carboxylase (ACC), actinin-1 (loading control), or measurement of 2-deoxy-D-[^{3}H]glucose uptake ($n = 5$ mice, Bas, Cch). EDL muscles from some mice were treated with Ins ($n = 2$, 10 nM, 20 min). Shown are representative immunoblots from 3 independent muscle lysates and mean results of glucose uptake as fold above basal for Cch ($P < 0.05$) and Ins. *D*: nicotinic acetylcholine receptors mediate the majority of the Cch response of the gain in cell surface GLUT4*myc* in C_2C_{12} myotubes. Myotube cultures were preincubated with bungarotoxin (BgTx; 125 nM, 30 min) or atropine (Atrop; 3 μM, 30 min) prior to incubation with Cch (100 μM, 20 min) or with no further additions (Bas; 30 min). Some cultures were incubated with the nicotinic acetylcholine receptor epibatidine (Epi; 100 nM, 30 min). Illustrated are the mean fold changes in cell surface GLUT4*myc* density relative to the basal condition from 3 to 4 experiments, $*P < 0.05$ and $\#\#P < 0.001$ relative to basal. BgTx significantly inhibited the carbachol response.

stimulated multiple contractions of individual myotubes for ≤20 min, and BTS completely inhibited carbachol-induced contractions in live C_2C_{12} myotube cultures (see Supplemental Videos; Supplemental Material for this article is available at the *AJP-Endocrinology and Metabolism* web site). BTS also caused profound inhibition of the carbachol-mediated phosphorylation of AMPK on Thr^{172} (Fig. 5*A*) and phosphorylation of ACC. As expected, BTS was without effect on the phosphorylation of AMPK and ACC in response to direct activation of AMPK by AICAR (Fig. 5*A*). Importantly, carbachol-stimulated cell surface GLUT4*myc* levels were inhibited 56.6 ± 0.1% by BTS, but BTS had no effect on AICAR-stimulated gain in cell surface GLUT4*myc* (Fig. 5*B*). Together, these data suggest that carbachol activates AMPK through force generation, and this accounts for a significant proportion of the carbachol-regulated GLUT4*myc* response.

Inhibition of AMPK reduces carbachol-induced increases in cell surface GLUT4. The AMPK inhibitor compound C effectively prevented phosphorylation of phospho-Ser^{79} ACC stimulated by either AICAR or carbachol (Fig. 6*A*). In addition, compound C largely prevented the AICAR- and carbachol-mediated rise in cell surface GLUT4*myc* by 79.6 ± 0.1 and

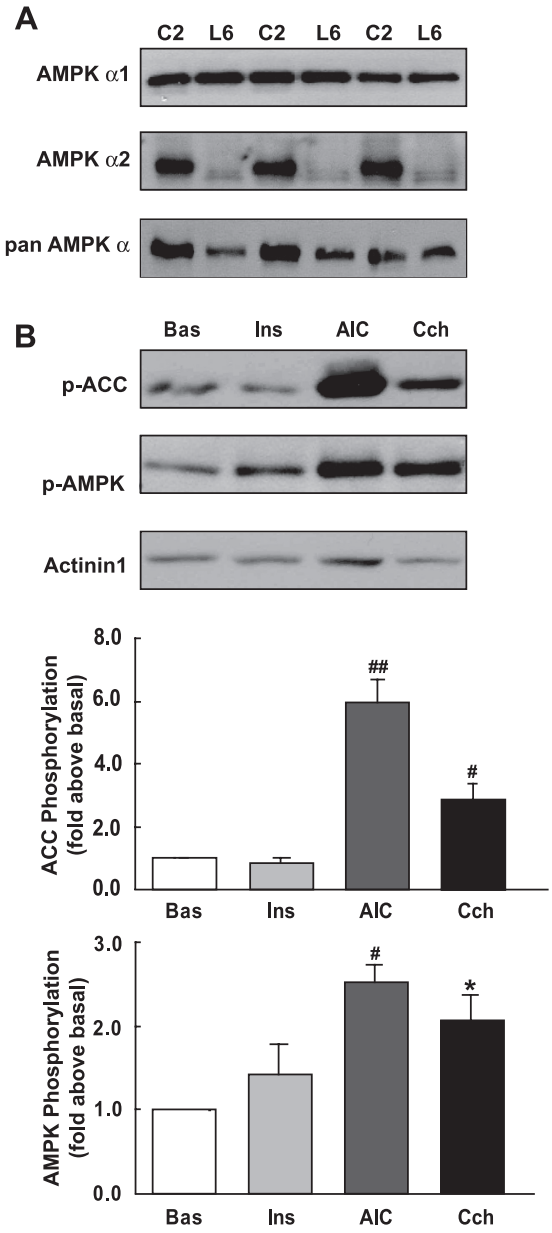

Fig. 4. Cch activates AMPK in C_2C_{12}-GLUT4*myc* myotubes. *A:* whole cell lysates were prepared from C_2C_{12}-GLUT4*myc* (C2) and L6-GLUT4*myc* (L6) myotube cultures, and equal protein amounts were immunoblotted with pan-α-subunit and α1- and α2-specific AMPK antibodies. Shown are immunoblots of at least 3 independently prepared lysates. *B*: C_2C_{12}-GLUT4*myc* myotubes were serum deprived for 4.5 h, including the incubation periods with Ins (10 nM, 10 min), AIC (2 mM, 60 min), or Cch (100 μM, 10 min) prior to whole cell lysates being processed for immunoblotting for p-Thr^{172} AMPK, p-Ser^{79} ACC, or actinin-1 (loading control). Shown is a representative immunoblot and the mean densitometry quantification, using Image J (NIH Image software), of at least 3 independent experiments of the fold change in p-Thr^{172} AMPK and p-Ser^{79} ACC relative to basal; *$P < 0.05$, #$P < 0.01$, and ##$P < 0.001$.

65.4 ± 0.1%, respectively (Fig. 6*B*). Of note, compound C did not inhibit insulin-stimulated GLUT4*myc* levels (data not shown). The extent of inhibition of carbachol-stimulated AMPK signaling and the gain in cell surface GLUT4*myc* by compound C suggests that carbachol generates signals through AMPK to mobilize GLUT4*myc*.

To further ascertain the participation of AMPK in the carbachol responses, we used siRNA to reduce expression of AMPKα1 and -α2 subunits simultaneously. By these means, the total AMPKα subunit content was lowered by 79.0 ± 0.1% (Fig. 7*A*), and the AICAR- or carbachol-stimulated gains in GLUT4*myc* cell surface levels were diminished significantly, by 36.0 ± 0.1 and 51.6 ± 0.1%, respectively (Fig. 7*B*). The remaining response could be due to residual AMPK signaling, as we observed for AICAR and carbachol (Fig. 7*A*), and/or to additional inputs participating in GLUT4 mobilization.

In skeletal muscle, LKB1 is the major upstream kinase of AMPK (36, 60) and regulates AMPK activity by phosphorylating the Thr^{172} regulatory site (18, 75). Thus, we used siRNA-mediated knockdown of LKB1 to explore its participation in carbachol signaling. By this approach, LKB1 expression was reduced by 84.0 ± 0.1% (Fig. 8*A*), and concomitantly there was a significant inhibition of the AICAR- or carbachol-dependent gains in cell surface GLUT4*myc*, by 42.6 ± 0.1 and 43.0 ± 0.1%, respectively (Fig. 8*B*). As with AMPKα subunit knockdown, the remaining responses to AICAR and carbachol may be ascribed to the remainder of LKB1 and AMPK signaling.

Carbachol raises intracellular calcium in C_2C_{12}-GLUT4myc myotubes. Intracellular calcium was the first signaling second messenger implicated in the stimulation of contraction-stimulated glucose uptake in skeletal muscle (22). Recently, using L6 muscle cell cultures, we showed that membrane depolarization by high extracellular potassium leads to a rise in

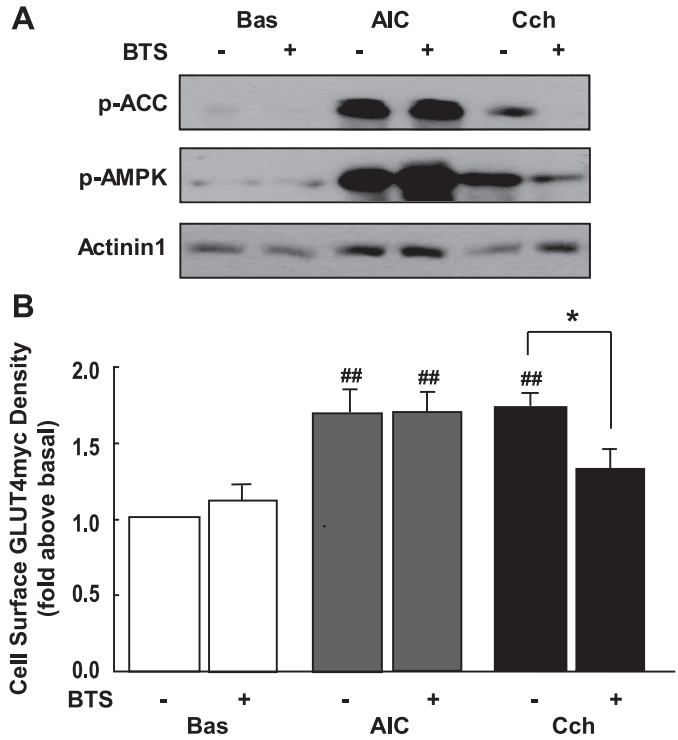

Fig. 5. Inhibition of myosin II ATPase reduces the gain in cell surface GLUT4*myc* induced by carbachol. C_2C_{12}-GLUT4*myc* myotubes were serum deprived for 4.5 h, including preincubation with or without the myosin II ATPase inhibitor *N*-benzyl-*p*-toluenesulfonamide (BTS; 50 μM, 30 min) prior to incubation with Cch (100 μM, 10 min prior to immunoblotting or 20 min prior to cell surface GLUT4*myc* measurement) or AIC (2 mM, 60 min). *A*: whole cell lysates were immunoblotted for p-Ser^{79} ACC, p-Thr^{172} AMPK, and actinin-1 (loading control). *B*: illustrated are the mean fold changes in cell surface GLUT4*myc* density induced by Cch in the absence (−) or presence (+) of BTS (relative to the basal condition; ##$P < 0.001$). BTS significantly inhibited the Cch response; *$P < 0.05$.

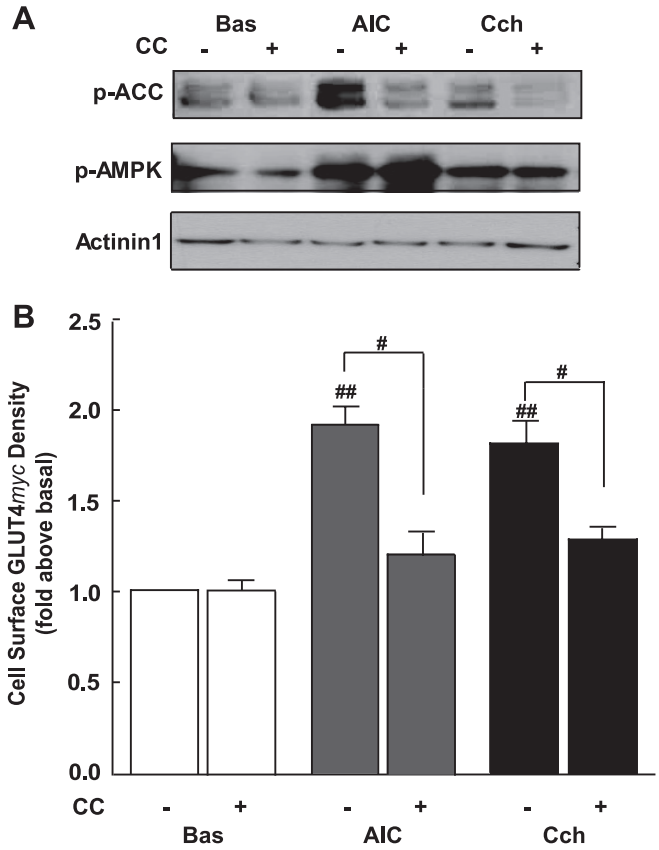

Fig. 6. Inhibition of AMPK with compound C (CC) reduces the gain in cell surface GLUT4*myc* induced by Cch. C_2C_{12}-GLUT4*myc* myotubes were serum deprived for 4.5 h, including preincubation with or without CC (10 μM, 30 min) prior to incubation with AIC (2 mM, 60 min) or Cch (100 μM, 10 min prior to immunoblotting or 20 min prior to cell surface GLUT4*myc* measurement). *A:* whole cell lysates were immunoblotted for p-Ser^{79} ACC, p-Thr^{172} AMPK, and actinin-1 (loading control). *B*: mean fold changes in cell surface GLUT4*myc* density induced by AIC or Cch in the absence (−) or presence (+) of CC (relative to the basal condition; ##$P < 0.001$). CC significantly inhibited the AIC and carbachol responses; #$P < 0.01$.

intracellular calcium and elevations in cell surface GLUT4 and glucose uptake (72). Interestingly, the effect of depolarization on glucose uptake was independent of AMPK in those cells, which also do not contract even when depolarized. In the present study, we find that activation of the acetylcholine receptors by carbachol induces a rise in intracellular calcium in C_2C_{12} myotubes (Fig. 9*A*). A dose of carbachol as low as 1 μM yielded a small rapid spike in intracellular calcium that recovered to near basal levels within 1 min. At 100 μM, carbachol caused iterative calcium cycling (Fig. 9*A*) that may be ascribed to ongoing calcium-induced calcium release and calcium reuptake by the sarcoplasmic reticulum. At 1 mM, carbachol induced a marked rise in intracellular calcium that slowly recovered to reach a stable increase of ~50% of the maximal response. The carbachol-elicited rise in surface GLUT4*myc* levels may require calcium, since preincubation of C_2C_{12}-GLUT4*myc* myotubes with the membrane permeant calcium chelator BAPTA-AM (Fig. 9*B*) reduced the carbachol response by 63.7 ± 0.2%. On the other hand, BAPTA-AM also inhibited contraction of carbachol-stimulated C_2C_{12} cultures (not shown).

How could cytosolic calcium signal to GLUT4? Recently, Jensen et al. (28) demonstrated that mild muscle contractions lead to phosphorylation of AMPKα1 and -α2 complexes in a CaMKK-dependent manner, and CaMKKβ is a newly recognized upstream kinase of the Thr^{172} site of AMPK catalytic α-subunits (19, 25, 74). Therefore, we explored the possible contribution of CaMKK signaling in carbachol-induced increases of cell surface GLUT4*myc*. C_2C_{12}-GLUT4*myc* myotubes express both CaMKKα and CaMKKβ isoforms (Fig. 10*A*), and the CaMKK inhibitor STO-609 reduced AMPK and ACC phosphorylation in both resting and carbachol-challenged cells (Fig. 10*B*). However, despite the reduction in basal AMPK and ACC phosphorylation, STO-609 did not significantly alter the fold stimulation of phosphorylation of either protein in response to carbachol (Fig. 10*C*). More precisely, carbachol induced a 1.9 ± 0.2- and 2.0 ± 0.1-fold phosphorylation of AMPK and ACC, respectively, in the absence of STO-609, and a 1.7 ± 0.2- and 2.0 ± 0.2-fold phosphorylation of AMPK and ACC, respectively, in the presence of STO-609 (Fig. 10*C*). Finally, STO-609 had no effect on the carbachol-stimulated rise in cell surface GLUT4*myc* (Fig. 10*D*). These results suggest that CaMKK does not play a role in carbachol-regulated GLUT4 traffic. Thus, carbachol raises intracellular calcium and may induce changes in GLUT4 traffic, but if so, they are not relayed via CaMKK signaling to AMPK and may instead involve other mechanisms. Interestingly, recent studies support a contribution of CaMKII in contraction-stimulated muscle glucose uptake (76, 77), and we have observed that a gain in surface levels of GLUT4*myc* is reduced partly by the CaMKII inhibitor KN-93 (data not shown). Whereas a separate, in-depth study is warranted to tease apart the calcium-dependent arm of signaling, the current study reveals that LKB1-AMPK and calcium are key elements in the mobilization of GLUT4 in response to carbachol in a cellular model of muscle contraction.

DISCUSSION

Contribution of AMPK to contraction-stimulated glucose uptake. Contraction-stimulated glucose uptake in muscle is an important physiological response that has far-reaching implications on whole body glucose homeostasis, insulin sensitivity, and type 2 diabetes (5, 17, 54, 73). Importantly, contraction-stimulated glucose uptake is not impaired in insulin-resistant states such as obesity and type 2 diabetes (47, 58, 68). Thus, a clear understanding of the regulation of glucose uptake by contraction signaling could form the basis of rational drug design for fast-acting stimulators of muscle glucose uptake. Numerous reports have demonstrated that AMPK has a role in contraction-induced signals that regulate muscle glucose uptake (29, 41, 45, 76, 77). However, the link between AMPK and muscle glucose uptake is complex and can depend on the muscle fiber type, AMPK subunit expression, exercise intensity, and the duration of the exercise (4, 30). Although the AMP mimetic AICAR activates AMPK and stimulates muscle glucose uptake, it does not fully recapitulate contraction-stimulated glucose uptake (31, 45) because mice null for the AMPKα2 catalytic subunit no longer display AICAR-stimulated muscle glucose uptake yet have normal contraction-stimulated glucose uptake (31). Furthermore, the skeletal muscle-specific expression of the K45R dominant-negative AMPKα2 mutant fully inhibits AICAR-stimulated glucose uptake, whereas its effect on the contraction response is partial (29, 41, 45). On the other hand, the use of AICAR provides proof of concept that AMPK can mediate regulation of GLUT4 and stimulate

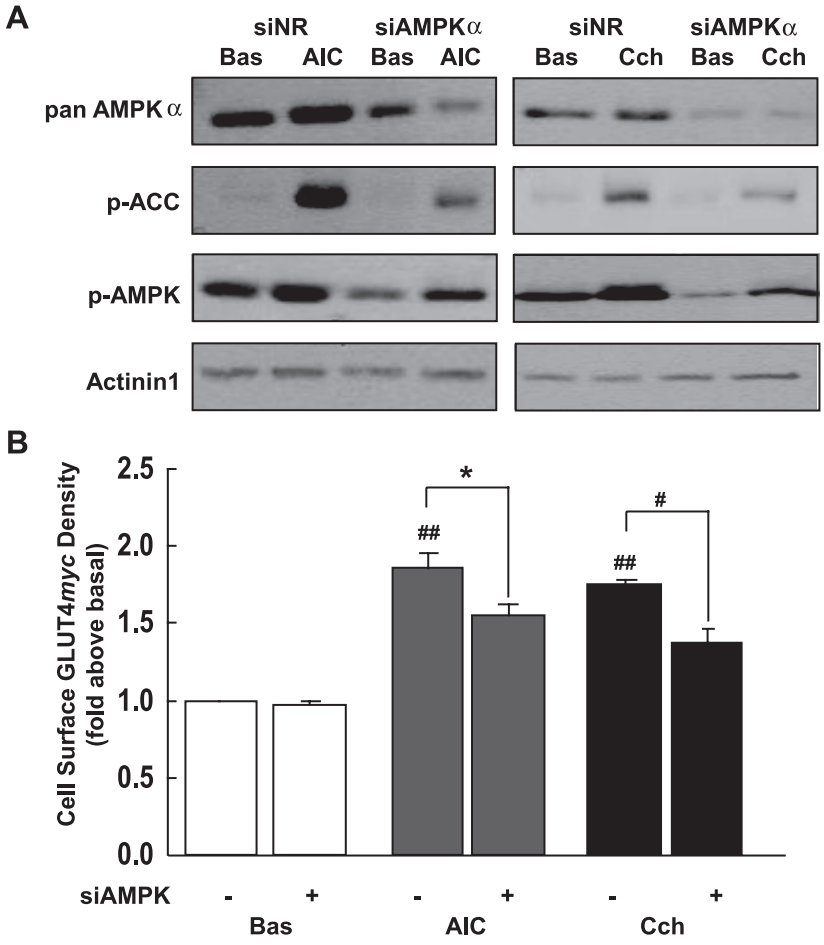

Fig. 7. RNAi-mediated knockdown of AMPK catalytic subunit expression reduces the gain in cell surface GLUT4*myc* induced by AIC and Cch. C_2C_{12}-GLUT4*myc* myotubes were transfected with siRNA oligomers (200 nM) to nonrelated (siNR) sequences or to the α1- and α2-catalytic subunits of AMPK (siAMPK) for 72 h prior to experimentation, as described in MATERIALS AND METHODS. Myotube cultures were serum deprived for 4.5 h, including the incubation with AIC (2 mM, 60 min) or Cch (100 μM, 10 min prior to immunoblotting or 20 min prior to cell surface GLUT4*myc* measurement). *A*: whole cell lysates from AIC- and carbachol-treated cultures were immunoblotted for pan-AMPKα, p-Ser^{79} ACC, p-Thr^{172} AMPK, and actinin-1. Shown are representative immunoblots of 3 independent experiments. *B*: illustrated are the mean fold changes in cell surface GLUT4*myc* density induced by AIC or carbachol in cultures treated with siNR (−) or siAMPK (+), as indicated, relative to the basal condition; ##$P < 0.001$. siAMPK significantly inhibited AIC and Cch responses; *$P < 0.05$ and #$P < 0.01$, respectively.

glucose uptake in muscle. The above literature analysis suggests that AMPK activation is sufficient but is not the only signal regulating glucose uptake in mature skeletal muscle, and it does not reveal the specific impact of contraction on GLUT4 per se.

Generation of a cell system amenable to contraction to elucidate signals regulating GLUT4 translocation. In the present study, we create an in vitro model of cultured C_2C_{12} muscle cells that overexpress GLUT4*myc* to evaluate the role of AMPK in regulating glucose uptake and GLUT4 traffic by direct activation (through AICAR) or via the more physiological route of acetylcholine receptor activation (through carbachol). We show that these effects of carbachol are mediated by the nicotinic acetylcholine receptor. We further demonstrate that inhibition of AMPK signaling with compound C, siRNA knockdown of both AMPK catalytic subunits, or LKB1 knockdown each point to involvement of AMPK in the AICAR- or carbachol-induced rise of cell surface GLUT4*myc*. GLUT4*myc* overexpression in C_2C_{12} myotubes improved the responsiveness of their glucose uptake to various stimuli, but there remains some input of GLUT1 to this response.

In skeletal muscle, LKB1 is the major activator of AMPK (60). Surprisingly, when this enzyme was knocked down in C_2C_{12} myotubes by 84.0 ± 0.1%, we still saw partial AICAR- or carbachol-induced phosphorylation of AMPK and ACC. These results suggest that the residual LKB1 suffices to partially activate AMPK signaling and GLUT4 traffic in response to AICAR and carbachol. Likewise, knockdown of AMPKα subunit expression by 79.0 ± 0.1% (as detected by a pan-AMPKα antibody) allowed significant carbachol- and AICAR-stimulated AMPK activation and partial gain in surface GLUT4*myc*. It is conceivable that a greater ablation of LKB1 and AMPK expression is required for complete elimination of signaling via the LKB1-AMPK module and abating GLUT4*myc* traffic. Animal studies indeed suggest that low levels of LKB1 activity suffice to allow effective signaling through this module. Indeed, marked depression of signaling is required to demonstrate that LKB1 plays a role in muscle glucose uptake (60).

Alternatively, the above results raise the possibility that the carbachol-induced rise in cytosolic calcium and its effectors may on their own stimulate AMPK in C_2C_{12} myotubes. It was important to test this possibility, since cytosolic calcium can activate AMPK via CaMKK in mature muscles (28). Moreover, low-intensity tetanic contraction of mouse soleus and EDL muscles stimulates AMPK activity and glucose uptake, responses that are inhibited partly by the CaMKK inhibitor STO-609 (28). However, this group has raised concerns regarding the specificity of STO-609 because the drug inhibited activation of the AMPKα2 isoform by contraction, a response held to be mostly LKB1 dependent (30). However, in C_2C_{12} myotubes, despite expressing both CaMKKα and -β isoforms, STO-609 did not affect carbachol-induced increases in GLUT4*myc* at the cell surface. STO-609 reduces the basal level of phosphorylation of AMPK and ACC, but in the

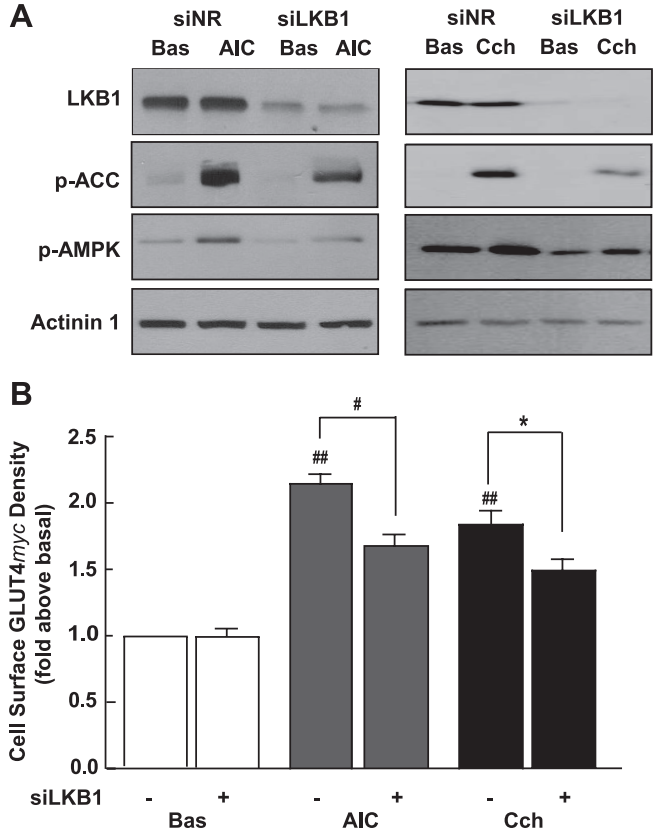

Fig. 8. RNAi-mediated knockdown of LKB1 expression reduces the gain in cell surface GLUT4*myc* induced by AIC and Cch. C_2C_{12}-GLUT4*myc* myotubes were transfected with siRNA oligomers (200 nM) to siNR sequences or to siAMPK for 72 h prior to experimentation, as described in MATERIALS AND METHODS. Myotube cultures were serum deprived for 4.5 h, including the incubation with AIC (2 mM, 60 min) or Cch (100 μM, 10 min prior to immunoblotting or 20 min prior to cell surface GLUT4*myc* measurement). *A*: whole cell lysates from AIC- and Cch-treated cultures were immunoblotted for LKB1, p-Ser^{79} ACC, p-Thr^{172} AMPK, and actinin-1. Shown are representative immunoblots of 5 independent experiments. *B*: illustrated are the mean fold changes in cell surface GLUT4*myc* density induced by AIC or Cch in cultures treated with siNR (−) or siLKB1 (+), as indicated, relative to the basal condition; ##$P < 0.001$. siLKB1 significantly inhibited AIC and Cch responses; #$P < 0.01$ and *$P < 0.05$, respectively.

presence of STO-609, carbachol still manages full (2-fold) stimulation of AMPK and ACC phosphorylation compared with the carbachol responses in its absence. Although calcium may lead to preferential activation of AMPKα1 complexes in skeletal muscle (27), we speculate in C_2C_{12} that calcium and CaMKK may regulate the basal activity of AMPKα1 complexes. Similarly, RNA interference of LKB1 expression still allows some stimulation of AMPK signaling by carbachol, but LKB1 is critically important for activation of AMPKα2 complexes in skeletal muscle (60). Future studies will test whether carbachol signaling shows specificity toward α2-complexes of AMPK.

Carbachol stimulation caused a rapid elevation in cytosolic calcium. Concomitantly, AMPK was activated, but this is likely through the contraction-dependent use of ATP and elevation in AMP levels and not by a change in intracellular calcium. This in turn would activate the LKB1-AMPK signaling module. This sequence of events is supported by the observation that the myosin II ATPase inhibitor BTS inhibited carbachol-induced AMPK activation and the cell surface gain in GLUT4*myc* without affecting these parameters in response to AICAR. BTS is expected to prevent the carbachol-triggered myosin-actin cross-bridge cycling responsible for C_2C_{12} myotube contraction and relaxation. Indeed, carbachol induces contraction of C_2C_{12} myotube cultures that is completely blocked by BTS. Importantly, in skeletal muscle, BTS does not affect the rise in intracellular calcium evoked by electrical stimulation of skeletal muscle (1, 6). Hence, the inhibition of carbachol-stimulated phospho-AMPK levels by BTS suggests that the carbachol-induced contractile force most likely raises AMP levels in contracting myotubes. Each attempt to inhibit carbachol-induced gains in cell surface GLUT4*myc* through manipulation of AMPK was not fully effective, leaving room to hypothesize that other signaling pathways may regulate GLUT4 traffic in response to carbachol. Whereas

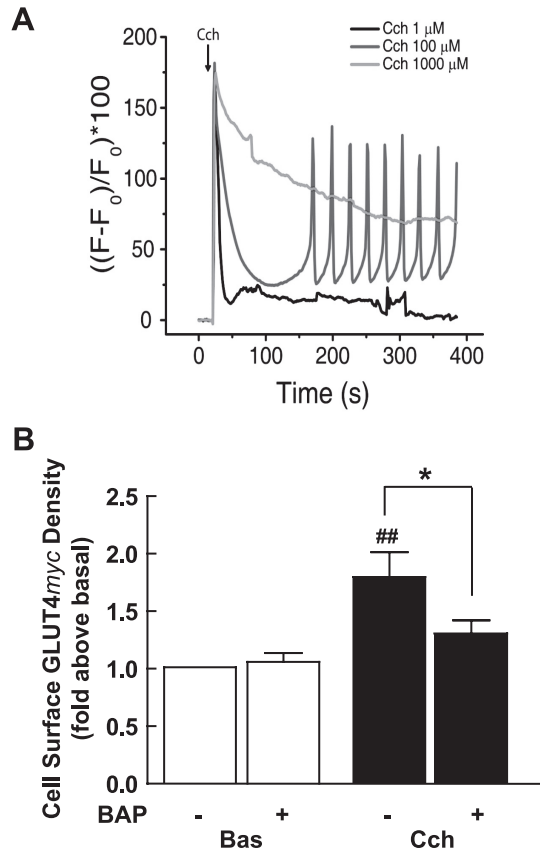

Fig. 9. Carbachol raises intracellular calcium in C_2C_{12}-GLUT4*myc* myotubes, and the maximum Cch-induced cell surface gain in GLUT4*myc* requires calcium. *A*: C_2C_{12}-GLUT4*myc* myotube cultures were grown on coverslips for live-cell analysis of intracellular calcium transients using Fluo 3-AM and fluorescence microscopy, as described in MATERIALS AND METHODS. Myotube cultures were loaded with Fluo 3-AM (10 μM, 50 min) prior to incubation with Cch at 1, 100, and 1,000 μM for the indicated time course. Changes in intracellular calcium-dependent fluorescence were plotted as the total relative fluorescence of Fluo 3 vs. time in seconds. Shown are representative traces of at least 5 independent experiments. *B*: chelation of intracellular calcium with BAPTA-AM (BAP) reduces the gain in cell surface GLUT4*myc* induced by carbachol. C_2C_{12}-GLUT4*myc* myotubes were serum deprived for 4.5 h, including the preincubation with BAP (15 μM, 15 min). Cultures were then treated with or without Cch (100 μM, 20 min). Illustrated are the mean fold changes in cell surface GLUT4*myc* density induced by Cch in 3 independent cultures treated without or with BAP; ##$P < 0.001$ relative to basal. BAP significantly inhibited the carbachol response; *$P < 0.05$.

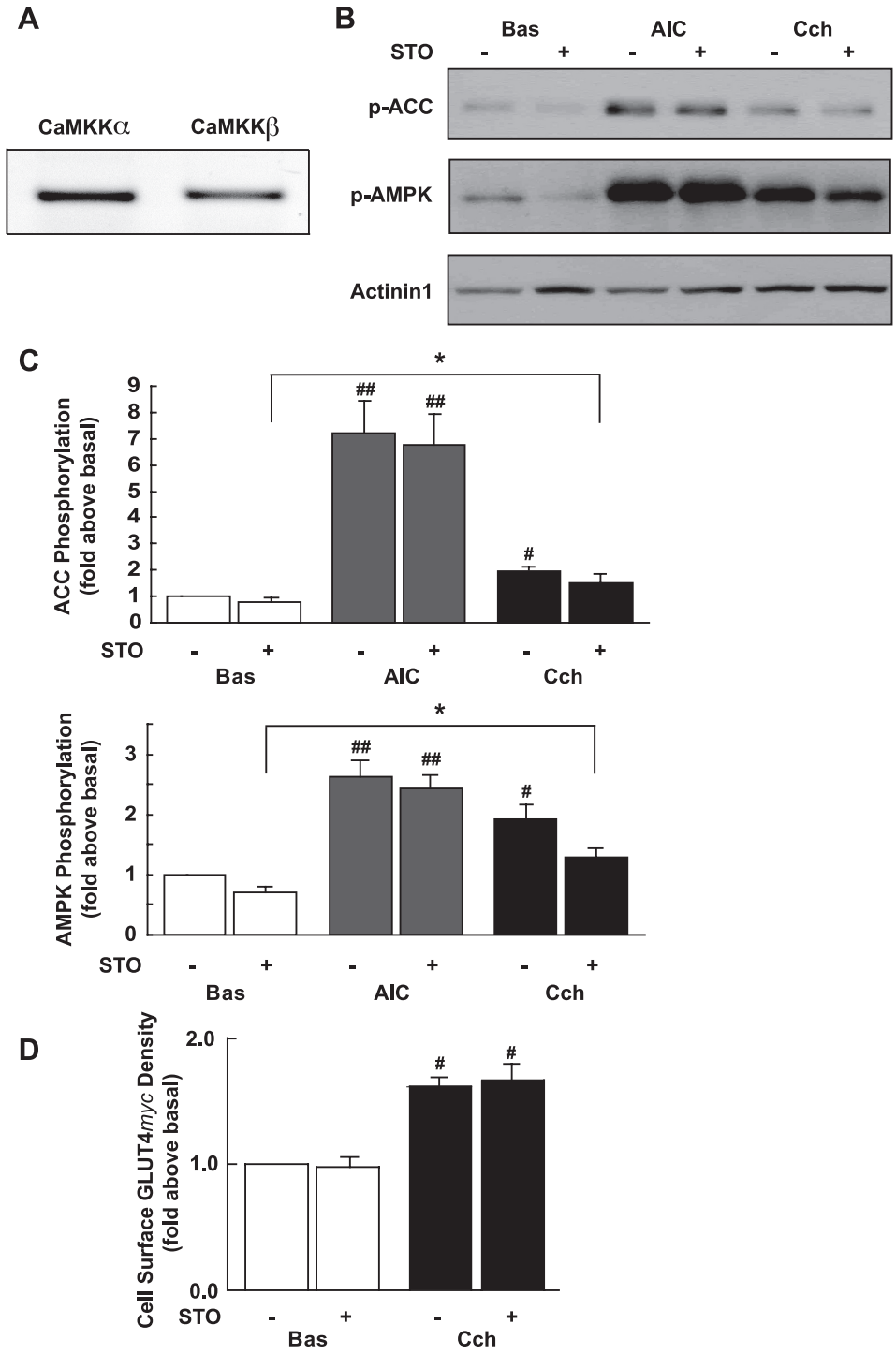

Fig. 10. The calmodulin kinase kinase inhibitor STO-609 (STO) does not affect the gain in cell surface GLUT4*myc* induced by Cch. *A*: total RNA was isolated from C_2C_{12}-GLUT4*myc* myotubes and used for RT-PCR detection of CaMKKα and CaMKKβ transcripts, as described in MATERIALS AND METHODS. *B–D*: myotube cultures were serum deprived for 4.5 h, including preincubation with or without STO (10 μM, 60 min), followed by incubation with Cch (100 μM, 10 min prior to immunoblotting or 20 min prior to cell surface GLUT4*myc* measurement) or AIC (2 mM, 60 min). Shown are representative whole cell lysates immunoblotted for p-Ser^{79} ACC and p-Thr^{172} AMPK (*B*). Densitometric quantification of p-Ser^{79} ACC and p-Thr^{172} AMPK levels from immunoblots; shown are the means from 8 to 12 independent experiments. #$P < 0.01$ or ##$P < 0.001$ compared with untreated basal. *$P < 0.05$ for Cch-stimulated cells pretreated with STO compared with unstimulated cells pretreated with STO (*C*). Myotube cultures were assayed for changes in cell surface density of GLUT4*myc* (*D*). Illustrated is the mean fold (representative of at least 6 experiments) cell surface GLUT4*myc* density induced by Cch in the absence (−) or presence (+) of STO relative to the basal condition; #$P <$ 0.01.

CaMKK is not a likely candidate, CaMKII may be, since KN93 partly interferes with carbachol-regulated GLUT4*myc* traffic.

Overall, our data support a model whereby carbachol produces contraction of C_2C_{12} myotube cultures, the consequential activation of the AMP-sensitive LKB1-AMPK signaling module, and this contributes to the elevation of GLUT4*myc* at the plasma membrane. Additional input into this response is mediated via the rise in cytosolic calcium, which, however, does not act on the CaMKK-AMPK signaling module. In future studies, we hope to uncover the calcium-dependent signaling pathway(s) that regulates GLUT4 traffic and glucose uptake in response to carbachol and other contraction-like stimuli.

How could AMPK and contraction regulate GLUT4 traffic? Recently, several laboratories have shown that contraction or AICAR administration leads to phosphorylation of the Rab-GAP AS160/Tbc1d4 in cultured cells (13, 67), rodent muscle (2, 38, 69), and human muscle (23, 64). This phosphorylation is AMPK dependent but Akt independent (38, 69). Interestingly, a mutant AS160 insensitive to negative regulation by upstream kinases reduced contraction-stimulated glucose up-

take when expressed in skeletal muscle (39). A related Rab-GAP, Tbc1d1, abundant in skeletal muscle, is also phosphorylated in response to AICAR and contraction in rodent muscle (12, 65). AS160/Tbc1d4 and Tbc1d1 are expressed in C_2C_{12} myotubes and become phosphorylated in response to carbachol and AICAR (Niu W, Bilan PJ, Ishikura S, and Klip A, unpublished observations). In future studies, we will define the roles of each of these proteins and their Rab-GTPase targets in the GLUT4 traffic in response to carbachol and other contraction-like stimuli.

In conclusion, muscle contraction in vivo and its stimulation of glucose uptake depend on multiple signaling pathways, including AMPK modules and a less-defined calcium-dependent mechanism. Progress in understanding this important physiological regulatory mechanism of glucose homeostasis has relied on studies of skeletal muscle tissue. Cultured cells are homogeneous and easily manipulated by using a variety of gene transfer and RNAi-mediated techniques. Yet to date, the study of contraction-stimulated glucose uptake does not benefit from a suitable in vitro model that would reveal paradigms subsequently testable in mature muscle. In the present study, we have characterized a C_2C_{12}-GLUT4*myc* cell line that responds to carbachol as a contraction-inducing stimulus. The observed carbachol-induced gain in cell surface GLUT4 recapitulates the contraction response in that it requires both AMPK- and calcium-dependent signals. Future work will focus on identifying the calcium-dependent signals and how signaling pathways interface with the GLUT4 traffic molecular machinery.

ACKNOWLEDGMENTS

We thank Benjamin E. Steinberg and Dave Mason for technical advice with live-cell light microscopy.

GRANTS

S. Ishikura was supported by a fellowship from the Banting and Best Diabetes Centre, University of Toronto. J. D. Schertzer was supported by fellowships from the Natural Sciences and Engineering Research Council of Canada and the Canadian Diabetes Association. A. Contreras-Ferrat was supported by a bilateral Canada-Chile short-term studentship from the Comision Nacional de Ciencia y Tecnologia (CONICYT), Chile.

This work was supported by a joint Canadian Institutes of Health Research and the National Natural Science Foundation of China (NSFC) grant to both A. Klip (no. FRN-82420) and W. Niu (no. 30611120532), by a NSFC grant (no. 30570912) to W. Niu, and by Tianjin Municipal Science and Technology Commission grants (nos. 09ZCZDSF04500 and 07JCZDJC07900) to W. Niu. Support to S. Lavandero came from CONICYT (FONDECYT Grant no. 1080436 and FONDAP Grant no. 15010006).

DISCLOSURES

No conflicts of interest are declared by the author(s).

REFERENCES

1. **Blair DR, Funai K, Schweitzer GG, Cartee GD.** A myosin II ATPase inhibitor reduces force production, glucose transport, and phosphorylation of AMPK and TBC1D1 in electrically stimulated rat skeletal muscle. *Am J Physiol Endocrinol Metab* 296: E993–E1002, 2009.
2. **Bruss MD, Arias EB, Lienhard GE, Cartee GD.** Increased phosphorylation of Akt substrate of 160 kDa (AS160) in rat skeletal muscle in response to insulin or contractile activity. *Diabetes* 54: 41–50, 2005.
3. **Carrasco MA, Marambio P, Jaimovich E.** Changes in IP3 metabolism during skeletal muscle development in vivo and in vitro. *Comp Biochem Physiol B Biochem Mol Biol* 116: 173–181, 1997.
4. **Cartee GD, Wojtaszewski JF.** Role of Akt substrate of 160 kDa in insulin-stimulated and contraction-stimulated glucose transport. *Appl Physiol Nutr Metab* 32: 557–566, 2007.
5. **Cartee GD, Young DA, Sleeper MD, Zierath J, Wallberg-Henriksson H, Holloszy JO.** Prolonged increase in insulin-stimulated glucose transport in muscle after exercise. *Am J Physiol Endocrinol Metab* 256: E494–E499, 1989.
6. **Cheung A, Dantzig JA, Hollingworth S, Baylor SM, Goldman YE, Mitchison TJ, Straight AF.** A small-molecule inhibitor of skeletal muscle myosin II. *Nat Cell Biol* 4: 83–88, 2002.
7. **Douen AG, Ramlal T, Rastogi S, Bilan PJ, Cartee GD, Vranic M, Holloszy JO, Klip A.** Exercise induces recruitment of the "insulin-responsive glucose transporter". Evidence for distinct intracellular insulin- and exercise-recruitable transporter pools in skeletal muscle. *J Biol Chem* 265: 13427–13430, 1990.
8. **Dugani CB, Randhawa VK, Cheng AW, Patel N, Klip A.** Selective regulation of the perinuclear distribution of glucose transporter 4 (GLUT4) by insulin signals in muscle cells. *Eur J Cell Biol* 87: 337–351, 2008.
9. **Eguez L, Lee A, Chavez JA, Miinea CP, Kane S, Lienhard GE, McGraw TE.** Full intracellular retention of GLUT4 requires AS160 Rab GTPase activating protein. *Cell Metab* 2: 263–272, 2005.
10. **Fujii N, Hirshman MF, Kane EM, Ho RC, Peter LE, Seifert MM, Goodyear LJ.** AMP-activated protein kinase alpha2 activity is not essential for contraction- and hyperosmolarity-induced glucose transport in skeletal muscle. *J Biol Chem* 280: 39033–39041, 2005.
11. **Fujita H, Nedachi T, Kanzaki M.** Accelerated de novo sarcomere assembly by electric pulse stimulation in C2C12 myotubes. *Exp Cell Res* 313: 1853–1865, 2007.
12. **Funai K, Cartee GD.** Contraction-stimulated glucose transport in rat skeletal muscle is sustained despite reversal of increased PAS-phosphorylation of AS160 and TBC1D1. *J Appl Physiol* 105: 1788–1795, 2008.
13. **Geraghty KM, Chen S, Harthill JE, Ibrahim AF, Toth R, Morrice NA, Vandermoere F, Moorhead GB, Hardie DG, MacKintosh C.** Regulation of multisite phosphorylation and 14-3-3 binding of AS160 in response to IGF-1, EGF, PMA and AICAR. *Biochem J* 407: 231–241, 2007.
14. **Goodyear LJ, King PA, Hirshman MF, Thompson CM, Horton ED, Horton ES.** Contractile activity increases plasma membrane glucose transporters in absence of insulin. *Am J Physiol Endocrinol Metab* 258: E667–E672, 1990.
15. **Hansen PA, Gulve EA, Holloszy JO.** Suitability of 2-deoxyglucose for in vitro measurement of glucose transport activity in skeletal muscle. *J Appl Physiol* 76: 979–985, 1994.
16. **Hawley JA, Hargreaves M, Zierath JR.** Signalling mechanisms in skeletal muscle: role in substrate selection and muscle adaptation. *Essays Biochem* 42: 1–12, 2006.
17. **Hawley JA, Lessard SJ.** Exercise training-induced improvements in insulin action. *Acta Physiol (Oxf)* 192: 127–135, 2008.
18. **Hawley SA, Boudeau J, Reid JL, Mustard KJ, Udd L, Mäkelä TP, Alessi DR, Hardie DG.** Complexes between the LKB1 tumor suppressor, STRAD alpha/beta and MO25 alpha/beta are upstream kinases in the AMP-activated protein kinase cascade. *J Biol* 2: 28, 2003.
19. **Hawley SA, Pan DA, Mustard KJ, Ross L, Bain J, Edelman AM, Frenguelli BG, Hardie DG.** Calmodulin-dependent protein kinase kinase-beta is an alternative upstream kinase for AMP-activated protein kinase. *Cell Metab* 2: 9–19, 2005.
20. **Hayashi T, Hirshman MF, Kurth EJ, Winder WW, Goodyear LJ.** Evidence for 5′ AMP-activated protein kinase mediation of the effect of muscle contraction on glucose transport. *Diabetes* 47: 1369–1373, 1998.
21. **Henning RH, Duin M, van Popta JP, Nelemans A, den Hertog A.** Different mechanisms of Ca2(+)-handling following nicotinic acetylcholine receptor stimulation, P2U-purinoceptor stimulation and K(+)-induced depolarization in C2C12 myotubes. *Br J Pharmacol* 117: 1785–1791, 1996.
22. **Holloszy JO.** A forty-year memoir of research on the regulation of glucose transport into muscle. *Am J Physiol Endocrinol Metab* 284: E453–E467, 2003.
23. **Howlett KF, Sakamoto K, Garnham A, Cameron-Smith D, Hargreaves M.** Resistance exercise and insulin regulate AS160 and interaction with 14-3-3 in human skeletal muscle. *Diabetes* 56: 1608–1614, 2007.
24. **Huang C, Somwar R, Patel N, Niu W, Torok D, Klip A.** Sustained exposure of L6 myotubes to high glucose and insulin decreases insulin-stimulated GLUT4 translocation but upregulates GLUT4 activity. *Diabetes* 51: 2090–2098, 2002.
25. **Hurley RL, Anderson KA, Franzone JM, Kemp BE, Means AR, Witters LA.** The Ca2+/calmodulin-dependent protein kinase kinases are

AMP-activated protein kinase kinases. *J Biol Chem* 280: 29060–29066, 2005.
26. **Ishikura S, Klip A.** Muscle cells engage Rab8A and myosin Vb in insulin-dependent GLUT4 translocation. *Am J Physiol Cell Physiol* 295: C1016–C1025, 2008.
27. **Jensen TE, Rose AJ, Hellsten Y, Wojtaszewski JF, Richter EA.** Caffeine-induced Ca^{2+} release increases AMPK-dependent glucose uptake in rodent soleus muscle. *Am J Physiol Endocrinol Metab* 293: E286–E292, 2007.
28. **Jensen TE, Rose AJ, Jørgensen SB, Brandt N, Schjerling P, Wojtaszewski JF, Richter EA.** Possible CaMKK-dependent regulation of AMPK phosphorylation and glucose uptake at the onset of mild tetanic skeletal muscle contraction. *Am J Physiol Endocrinol Metab* 292: E1308–E1317, 2007.
29. **Jensen TE, Schjerling P, Viollet B, Wojtaszewski JF, Richter EA.** AMPK alpha1 activation is required for stimulation of glucose uptake by twitch contraction, but not by H2O2, in mouse skeletal muscle. *PLoS One* 3: e2102, 2008.
30. **Jensen TE, Wojtaszewski JF, Richter EA.** AMP-activated protein kinase in contraction regulation of skeletal muscle metabolism: necessary and/or sufficient? *Acta Physiol (Oxf)* 196: 155–174, 2009.
31. **Jørgensen SB, Viollet B, Andreelli F, Frøsig C, Birk JB, Schjerling P, Vaulont S, Richter EA, Wojtaszewski JF.** Knockout of the alpha2 but not alpha1 5′-AMP-activated protein kinase isoform abolishes 5-amino-imidazole-4-carboxamide-1-beta-4-ribofuranosidebut not contraction-induced glucose uptake in skeletal muscle. *J Biol Chem* 279: 1070–1079, 2004.
32. **Kanai F, Nishioka Y, Hayashi H, Kamohara S, Todaka M, Ebina Y.** Direct demonstration of insulin-induced GLUT4 translocation to the surface of intact cells by insertion of a c-myc epitope into an exofacial GLUT4 domain. *J Biol Chem* 268: 14523–14526, 1993.
33. **Kandror KV, Pilch PF.** Multiple endosomal recycling pathways in rat adipose cells. *Biochem J* 331: 829–835, 1998.
34. **Kane S, Sano H, Liu SC, Asara JM, Lane WS, Garner CC, Lienhard GE.** A method to identify serine kinase substrates. Akt phosphorylates a novel adipocyte protein with a Rab GTPase-activating protein (GAP) domain. *J Biol Chem* 277: 22115–22118, 2002.
35. **Kishi K, Muromoto N, Nakaya Y, Miyata I, Hagi A, Hayashi H, Ebina Y.** Bradykinin directly triggers GLUT4 translocation via an insulin-independent pathway. *Diabetes* 47: 550–558, 1998.
36. **Koh HJ, Arnolds DE, Fujii N, Tran TT, Rogers MJ, Jessen N, Li Y, Liew CW, Ho RC, Hirshman MF, Kulkarni RN, Kahn CR, Goodyear LJ.** Skeletal muscle-selective knockout of LKB1 increases insulin sensitivity, improves glucose homeostasis, and decreases TRB3. *Mol Cell Biol* 26: 8217–8227, 2006.
37. **Kotliar N, Pilch PF.** Expression of the glucose transporter isoform GLUT 4 is insufficient to confer insulin-regulatable hexose uptake to cultured muscle cells. *Mol Endocrinol* 6: 337–345, 1992.
38. **Kramer HF, Witczak CA, Fujii N, Jessen N, Taylor EB, Arnolds DE, Sakamoto K, Hirshman MF, Goodyear LJ.** Distinct signals regulate AS160 phosphorylation in response to insulin, AICAR, and contraction in mouse skeletal muscle. *Diabetes* 55: 2067–2076, 2006.
39. **Kramer HF, Witczak CA, Taylor EB, Fujii N, Hirshman MF, Goodyear LJ.** AS160 regulates insulin- and contraction-stimulated glucose uptake in mouse skeletal muscle. *J Biol Chem* 281: 31478–31485, 2006.
40. **Larance M, Ramm G, Stöckli J, van Dam EM, Winata S, Wasinger V, Simpson F, Graham M, Junutula JR, Guilhaus M, James DE.** Characterization of the role of the Rab GTPase-activating protein AS160 in insulin-regulated GLUT4 trafficking. *J Biol Chem* 280: 37803–37813, 2005.
41. **Lefort N, St.-Amand E, Morasse S, Côté CH, Marette A.** The α-subunit of AMPK is essential for submaximal contraction-mediated glucose transport in skeletal muscle in vitro. *Am J Physiol Endocrinol Metab* 295: E1447–E1454, 2008.
42. **Lin BZ, Pilch PF, Kandror K.** Sortilin is a major protein component of Glut4-containing vesicles. *J Biol Chem* 272: 24145–24147, 1997.
43. **McMahon DK, Anderson PA, Nassar R, Bunting JB, Saba Z, Oakeley AE, Malouf NN.** C_2C_{12} cells: biophysical, biochemical, and immunocytochemical properties. *Am J Physiol Cell Physiol* 266: C1795–C1802, 1994.
44. **Merrill GF, Kurth EJ, Hardie DG, Winder WW.** AICA riboside increases AMP-activated protein kinase, fatty acid oxidation, and glucose uptake in rat muscle. *Am J Physiol Endocrinol Metab* 273: E1107–E1112, 1997.
45. **Mu J, Brozinick JT, Valladares O, Bucan M, Birnbaum MJ.** A role for AMP-activated protein kinase in contraction- and hypoxia-regulated glucose transport in skeletal muscle. *Mol Cell* 7: 1085–1094, 2001.
46. **Murata H, Hruz PW, Mueckler M.** Indinavir inhibits the glucose transporter isoform Glut4 at physiologic concentrations. *AIDS* 16: 859–863, 2002.
47. **Musi N, Fujii N, Hirshman MF, Ekberg I, Fröberg S, Ljungqvist O, Thorell A, Goodyear LJ.** AMP-activated protein kinase (AMPK) is activated in muscle of subjects with type 2 diabetes during exercise. *Diabetes* 50: 921–927, 2001.
48. **Musi N, Hayashi T, Fujii N, Hirshman MF, Witters LA, Goodyear LJ.** AMP-activated protein kinase activity and glucose uptake in rat skeletal muscle. *Am J Physiol Endocrinol Metab* 280: E677–E684, 2001.
49. **Nedachi T, Fujita H, Kanzaki M.** Contractile C_2C_{12} myotube model for studying exercise-inducible responses in skeletal muscle. *Am J Physiol Endocrinol Metab* 295: E1191–E1204, 2008.
50. **Niu W, Huang C, Nawaz Z, Levy M, Somwar R, Li D, Bilan PJ, Klip A.** Maturation of the regulation of GLUT4 activity by p38 MAPK during L6 cell myogenesis. *J Biol Chem* 278: 17953–17962, 2003.
51. **Paulson HL, Claudio T.** Temperature-sensitive expression of all-Torpedo and Torpedo-rat hybrid AChR in mammalian muscle cells. *J Cell Biol* 110: 1705–1717, 1990.
52. **Randhawa VK, Bilan PJ, Khayat ZA, Daneman N, Liu Z, Ramlal T, Volchuk A, Peng XR, Coppola T, Regazzi R, Trimble WS, Klip A.** VAMP2, but not VAMP3/cellubrevin, mediates insulin-dependent incorporation of GLUT4 into the plasma membrane of L6 myoblasts. *Mol Biol Cell* 11: 2403–2417, 2000.
53. **Randhawa VK, Thong FS, Lim DY, Li D, Garg RR, Rudge R, Galli T, Rudich A, Klip A.** Insulin and hypertonicity recruit GLUT4 to the plasma membrane of muscle cells by using N-ethylmaleimide-sensitive factor-dependent SNARE mechanisms but different v-SNAREs: role of TI-VAMP. *Mol Biol Cell* 15: 5565–5573, 2004.
54. **Rockl KS, Witczak CA, Goodyear LJ.** Signaling mechanisms in skeletal muscle: acute responses and chronic adaptations to exercise. *IUBMB Life* 60: 145–153, 2008.
55. **Rose AJ, Richter EA.** Skeletal muscle glucose uptake during exercise: how is it regulated? *Physiology (Bethesda)* 20: 260–270, 2005.
56. **Rudich A, Klip A.** Push/pull mechanisms of GLUT4 traffic in muscle cells. *Acta Physiol Scand* 178: 297–308, 2003.
57. **Rudich A, Konrad D, Torok D, Ben-Romano R, Huang C, Niu W, Garg RR, Wijesekara N, Germinario RJ, Bilan PJ, Klip A.** Indinavir uncovers different contributions of GLUT4 and GLUT1 towards glucose uptake in muscle and fat cells and tissues. *Diabetologia* 46: 649–658, 2003.
58. **Ryder JW, Gilbert M, Zierath JR.** Skeletal muscle and insulin sensitivity: pathophysiological alterations. *Front Biosci* 6: D154–D163, 2001.
59. **Sakamoto K, Göransson O, Hardie DG, Alessi DR.** Activity of LKB1 and AMPK-related kinases in skeletal muscle: effects of contraction, phenformin, and AICAR. *Am J Physiol Endocrinol Metab* 287: E310–E317, 2004.
60. **Sakamoto K, McCarthy A, Smith D, Green KA, Grahame Hardie D, Ashworth A, Alessi DR.** Deficiency of LKB1 in skeletal muscle prevents AMPK activation and glucose uptake during contraction. *EMBO J* 24: 1810–1820, 2005.
61. **Sargeant RJ, Paquet MR.** Effect of insulin on the rates of synthesis and degradation of GLUT1 and GLUT4 glucose transporters in 3T3-L1 adipocytes. *Biochem J* 290: 913–919, 1993.
62. **Schertzer JD, Gehrig SM, Ryall JG, Lynch GS.** Modulation of insulin-like growth factor (IGF)-I and IGF-binding protein interactions enhances skeletal muscle regeneration and ameliorates the dystrophic pathology in mdx mice. *Am J Pathol* 171: 1180–1188, 2007.
63. **Shi J, Kandror KV.** Sortilin is essential and sufficient for the formation of Glut4 storage vesicles in 3T3-L1 adipocytes. *Dev Cell* 9: 99–108, 2005.
64. **Sriwijitkamol A, Coletta DK, Wajcberg E, Balbontin GB, Reyna SM, Barrientes J, Eagan PA, Jenkinson CP, Cersosimo E, DeFronzo RA, Sakamoto K, Musi N.** Effect of acute exercise on AMPK signaling in skeletal muscle of subjects with type 2 diabetes: a time-course and dose-response study. *Diabetes* 56: 836–848, 2007.
65. **Taylor EB, An D, Kramer HF, Yu H, Fujii NL, Roeckl KS, Bowles N, Hirshman MF, Xie J, Feener EP, Goodyear LJ.** Discovery of TBC1D1 as an insulin-, AICAR-, and contraction-stimulated signaling nexus in mouse skeletal muscle. *J Biol Chem* 283: 9787–9796, 2008.

66. **Teplov AY, Grishin SN, Zefirov AL.** Possible mechanisms for the effect of protein sensitization on contractile function of fast and slow muscles in mice. *Bull Exp Biol Med* 147: 560–563, 2009.
67. **Thong FS, Bilan PJ, Klip A.** The Rab GTPase-activating protein AS160 integrates Akt, protein kinase C, and AMP-activated protein kinase signals regulating GLUT4 traffic. *Diabetes* 56: 414–423, 2007.
68. **Thyfault JP, Cree MG, Zheng D, Zwetsloot JJ, Tapscott EB, Koves TR, Ilkayeva O, Wolfe RR, Muoio DM, Dohm GL.** Contraction of insulin-resistant muscle normalizes insulin action in association with increased mitochondrial activity and fatty acid catabolism. *Am J Physiol Cell Physiol* 292: C729–C739, 2007.
69. **Treebak JT, Glund S, Deshmukh A, Klein DK, Long YC, Jensen TE, Jorgensen SB, Viollet B, Andersson L, Neumann D, Wallimann T, Richter EA, Chibalin AV, Zierath JR, Wojtaszewski JF.** AMPK-mediated AS160 phosphorylation in skeletal muscle is dependent on AMPK catalytic and regulatory subunits. *Diabetes* 55: 2051–2058, 2006.
70. **Wang Q, Khayat Z, Kishi K, Ebina Y, Klip A.** GLUT4 translocation by insulin in intact muscle cells: detection by a fast and quantitative assay. *FEBS Lett* 427: 193–197, 1998.
71. **Weston CA, Teressa G, Weeks BS, Prives J.** Agrin and laminin induce acetylcholine receptor clustering by convergent, Rho GTPase-dependent signaling pathways. *J Cell Sci* 120: 868–875, 2007.
72. **Wijesekara N, Tung A, Thong F, Klip A.** Muscle cell depolarization induces a gain in surface GLUT4 via reduced endocytosis independently of AMPK. *Am J Physiol Endocrinol Metab* 290: E1276–E1286, 2006.
73. **Wojtaszewski JF, Hansen BF, Gade J, Kiens B, Markuns JF, Goodyear LJ, Richter EA.** Insulin signaling and insulin sensitivity after exercise in human skeletal muscle. *Diabetes* 49: 325–331, 2000.
74. **Woods A, Dickerson K, Heath R, Hong SP, Momcilovic M, Johnstone SR, Carlson M, Carling D.** Ca2+/calmodulin-dependent protein kinase kinase-beta acts upstream of AMP-activated protein kinase in mammalian cells. *Cell Metab* 2: 21–33, 2005.
75. **Woods A, Johnstone SR, Dickerson K, Leiper FC, Fryer LG, Neumann D, Schlattner U, Wallimann T, Carlson M, Carling D.** LKB1 is the upstream kinase in the AMP-activated protein kinase cascade. *Curr Biol* 13: 2004–2008, 2003.
76. **Wright DC, Geiger PC, Holloszy JO, Han DH.** Contraction- and hypoxia-stimulated glucose transport is mediated by a Ca^{2+}-dependent mechanism in slow-twitch rat soleus muscle. *Am J Physiol Endocrinol Metab* 288: E1062–E1066, 2005.
77. **Wright DC, Hucker KA, Holloszy JO, Han DH.** Ca2+ and AMPK both mediate stimulation of glucose transport by muscle contractions. *Diabetes* 53: 330–335, 2004.
78. **Zaid H, Antonescu CN, Randhawa VK, Klip A.** Insulin action on glucose transporters through molecular switches, tracks and tethers. *Biochem J* 413: 201–215, 2008.